Organization and Development of Brain Stem Auditory Nuclei of the Chicken: Dendritic Gradients in Nucleus Laminaris

DANIEL J. SMITH AND EDWIN W RUBEL
Neuroscience Program and Departments of Otolaryngology and Physiology, University of Virginia Medical Center, Charlottesville, Virginia 22908

ABSTRACT Nucleus laminaris (NL) is a third-order auditory nucleus in the avian brain stem which receives spatially-segregated binaural inputs from the second-order magnocellular nuclei. The organization of dendritic structure in NL was examined in Golgi-impregnated brains from hatchling chickens. Quantitative analyses of dendritic size and number were made from camera lucida drawings of 135 neurons sampled from throughout the nucleus.

The most significant results of this study may be summarized as follows:

(1) The preponderant neuron in n. laminaris may be characterized as having a cylindrical-to-ovoid cell body, about 20 μm in diameter. The neurons comprising NL were found to be nearly completely homogeneous in issuing their dendrites in a bipolar fashion: one group of dendrites is clustered on the dorsal surface of the cells, the other group on the ventral. The dendrites of NL are contained within the glia-free neuropil surrounding the nucleus. From the rostromedial to the caudolateral poles of NL there is a gradient of increasing extension of the dendrites, increasing number of tertiary and higher-order dendrites, and increasing distance from the somata of the occurrence of branching.

(2) The total dendritic size (sum of the dorsal and ventral dendritic lengths of the cells) increases 3-fold from the rostromedial to the caudolateral poles of NL. About 50% of the variance in dendritic size is accounted for by the position of the cells in NL, and the gradient of dendritic size increase has the same orientation across NL as the tonotopic gradient of decreasing characteristic frequency in NL.

(3) From the rostromedial pole to the caudolateral pole of NL there is an 11-fold decrease in the number of primary dendrites along a gradient coinciding with the length and frequency gradients. Sixty-six percent of the variance in dendrite number is accounted for by position in the nucleus.

(4) The correlation of dorsal and ventral dendritic size on a cell-by-cell basis is not high ($r = 0.47$), indicating a fair amount of variability on the single-cell level. On the other hand, the average dorsal dendritic length within an isofrequency band in NL correlates very highly with the average ventral dendritic length. Thus, on an areal basis, the amount of dendritic surface area offered to the dorsal and ventral afferents is tightly regulated.

(5) The dorsal and ventral dendrites have separate gradients of increasing length and number across NL. The dorsal gradients are skewed toward the rostrocaudal axis, while the ventral dendritic gradients are skewed mediolaterally.

(6) There was no correlation between either dendritic size or number of primary dendrites and the size of the somata in NL, which remains relatively constant throughout the nucleus.

Several hypotheses about the ontogenetic control of dendritic structure are examined in light of the above data. Of these, the hypotheses that the ontogeny of dendritic size and number is largely under afferent control receives a great deal of circumstantial support.

Increasing interest in the avian auditory system has been sparked by a number of fields. Birds have been widely used for study of vocal communication (Hinde, '69) and this has led to study of the auditory neurophysiology underlying the acoustic communication (Schwartzkopff, '68; Konishi, '70; Sachs et al., '74; Rubel and Parks, '75; Leppelsack and Vogt, '76; Scheich '77; Sachs and Sinnott, '78) as well as of the ontogeny of vocal communication (Marler, '70; Marler and Waser, '77). The roles of audition in avian development (Vince, '69; Woolf et al., '76), especially perceptual development (Gottlieb, '71, '76; Rubel and Rosenthal, '75; Kerr et al., '79) have given impetus to studies of the functional and anatomical development of the avian auditory system (Konishi, '73; Saunders et al., '73; Rubel et al., '76; Hirokawa, '78; Jackson and Rubel, '78; Jackson, '78; Parks, '79; Jhaveri, '78). Finally, the unique phylogenetic position of Aves as the other major class evolving from reptiles has led to insights into the possible origins of mammalian neural structures (Bock, '69; Boord, '69; Nauta and Karten, '70; Jenkins and Masterson, '79) and to a better understanding of the avian auditory pathways (Boord, '61, '68; Boord and Rasmussen, '63; Karten, '67, '68; Leibler, '75; Parks and Rubel, '78).

In the avian brain stem, nucleus laminaris (NL) is composed of a sheet of cells between a dorsal and a ventral neuropil zone. Cytoarchitectonically the nucleus is quite homogeneous (Boord, '69). The major sources of the afferent supply to NL are from the ipsi- and contralateral nucleus magnocellularis (NM), a second-order auditory nucleus (Ramón y Cajal, '08; Boord, '68; Parks and Rubel, '75). Axons from NM branch and send one collateral to the dorsal neuropil of the ipsilateral NL, and the other collateral to the ventral neuropil of the contralateral NL (Rubel et al., '78; Jhaveri, '78), resulting in a spatially-segregated binaural input to NL.

Electrophysiological investigation of n. laminaris reveals that units are binaurally activated and quite homogeneous in their response properties, with no evidence of inhibitory interactions between stimuli applied to the two ears (Rubel and Parks, '75; Jackson et al., '78). NL is organized tonotopically; units with high characteristic frequencies are found at the rostromedial pole of the nucleus, and units responding to progressively lower frequencies are found progressively caudolaterad in NL. Thus, NL appears to be organized as a series of isofrequency bands, each running orthogonal to the tonotopic gradient and decreasing in frequency from the rostromedial to the caudolateral poles of the nucleus. The cartesian position of a cell in NL is an excellent predictor of its characteristic frequency, accounting for about 89% of the variance.

The purpose of the present study was to provide a thorough qualitative and quantitative analysis of dendritic morphology in NL of the hatchling chicken; such an analysis provides the necessary foundation for understanding the results of manipulating the ontogenetic milieu. In particular, the finding of graded changes in neuropil volume within NL (Rubel et al., '76) and observations by Ramón y Cajal ('08) suggested the possibility of a systematic change in dendrite morphology associated with the frequency organization of NL. Also, since the dorsal and ventral dendritic regions of NL receive matching binaural input it was of interest to determine if the dorsal and ventral dendritic processes of NL neurons are structurally similar. These possibilities were investigated, using the Golgi technique and quantitative analysis of camera lucida drawings. In addition, in the course of this study observations were made of the organization of the dendritic structure of NL which provide important clues to its developmental history.

METHODS

Qualitative observations were made on 47 White Leghorn chicken brains ranging in age at sacrifice from posthatch day 1 to day 25, stained with Golgi-Cox and Golgi-Kopsch methods. A few brains stained with the rapid Golgi techniques were also examined. Brains were embedded in celloidin and sectioned in the coronal or sagittal planes at 100-250 μm.

For the quantitative analyses, four brains sacrificed at five days posthatch and stained with a modification of the del Río Hortega-Golgi method (Stensaas, '67) were examined. These brains were embedded in celloidin and sectioned in the coronal plane at 180-240 μm. Sections were cleared in terpineol overnight and mounted in Permount. Several criteria were used to select the cells to be drawn. First, the cell had to be in NL. This was easily determined due to the distinctive morphology of NL cells, and the appearance of encapsulating fibers around the nucleus. Second, the cells had to appear fully impregnated. In the brains chosen, the impregnation of all cells in the sec-

tion appeared complete. Third, all of the dendritic processes had to appear in a single section. The thickness of the sections were such that this criterion eliminated only a few cells. Fourth, the processes had to be unambiguously resolvable throughout their lengths. In all, 135 cells were drawn at final magnifications of 540 ×, 825 ×, 1,325 ×, or 3,330 ×.

In order to provide a predictive map of dendritic structure in NL, and to relate these findings to our previous work, the position of each neuron which was drawn was determined in a manner similar to that used by Rubel and Parks ('75). Each serial section containing NL was drawn at low magnification (215 ×) with a camera lucida and every cell visible in the nucleus was drawn. The boundaries of the nucleus were determined by observation of the cellular morphology and of the encapsulating fiber tract which surrounds the nucleus. The distances of the medial and lateral edges of the nucleus from the midline were determined along a line orthogonal to the midline. The total lateral to medial extent of the nucleus (in micrometers), as taken from all sections of each individual nucleus, was set at 100%. Individual cell positions were projected at right angles onto the line orthogonal to the midline, and expressed as a percentage of the total lateral to medial (L-M) extent. The caudorostral position of the cells was determined in a similar fashion, with the total posterior to anterior (P-A) extent of NL set to 100%, and the (P-A) position of each cell determined by taking its cumulative depth into the nucleus from the posterior pole. This results in each cell being assigned a 2-point positional coordinate (%P-A, %L-M) on a planar projection of the nucleus in the horizontal plane. This manner of expressing position as a percentage of the total extent of the nucleus along each axis compensates for variation in the extent of NL across different animals, and was used in our previous investigations of the functional organization and development of NM and NL (Rubel and Parks, '75; Parks and Rubel, '75; Rubel et al., '76). Thus, results of different studies, whether using different methodologies or different ages, can be compared.

For an independent measure of the accuracy of the planar projections determined from the Golgi sections, a mean composite planar projection of NL was made. Three chickens, ten days of age, were perfused with 2% glutaraldehyde-2% formaldehyde. The brains were embedded in celloidin, sectioned at 14 μm, and stained with thionin. N. laminaris on both sides was then drawn by camera lucida from every third section, and a planar projection for each nucleus (6 in all) was made. At every tenth percentile on the P-A dimension, the mean L-M extent of the planar projections was determined, and a mean composite planar projection of NL was constructed (fig. 9).[1]

The drawings of NL cells were of two kinds. In the first, drawn to measure longitudinal area of dendrites, the cell bodies and processes were drawn in outline under camera lucida, employing a 100 × objective (n.a. = 1.3), at a final magnification of 3,300 ×. In these drawings, each dendrite was drawn separately (fig. 10B), in a series of segments, so that all parts of the dendrite were magnified equally. In the second type of drawing, to measure dendritic length, lines were drawn down the center of the dendrites throughout their extent, with branch points represented as nodes (fig. 10C). Care was taken in all drawings to insure equal magnification in all parts of the field. From the drawings for each cell, measurements were made of the dendritic area or length, for the combined dorsal and the combined ventral dendritic arborizations, with the aid of a digital planimeter (Numonics, Inc.). Since each drawing was individually scaled, the measurements were converted to micrometers or micrometers[2] for comparisons.

Bivariate and multivariate regression analyses were run using SPSS programs, on a CDC Cyber 170 computer. A linear model for the regressions was employed in all instances, as no greater correlative value was found for any regression employing logarithmic or power-function models.

RESULTS

Qualitative observations

In Nissl-stained sections, n. laminaris is a single monolayer of cell bodies bordered dorsad and ventrad by a clear, relatively cell-free area of neuropil. This neuropil zone is in turn delineated in extent by a layer rich in small glial cell bodies. In Golgi-Cox sections counter-stained with cresylviolet, the extent of the dendrites of NL neurons was found to be bounded by this glia-rich zone (fig. 1). Thus the dendritic regions of these cells are quite circumscribed and easily delineated.

Qualitative observations were drawn largely from brains stained with Golgi-Kopsch

[1] See Rubel and Parks ('75) for a further discussion of the planar projection method.

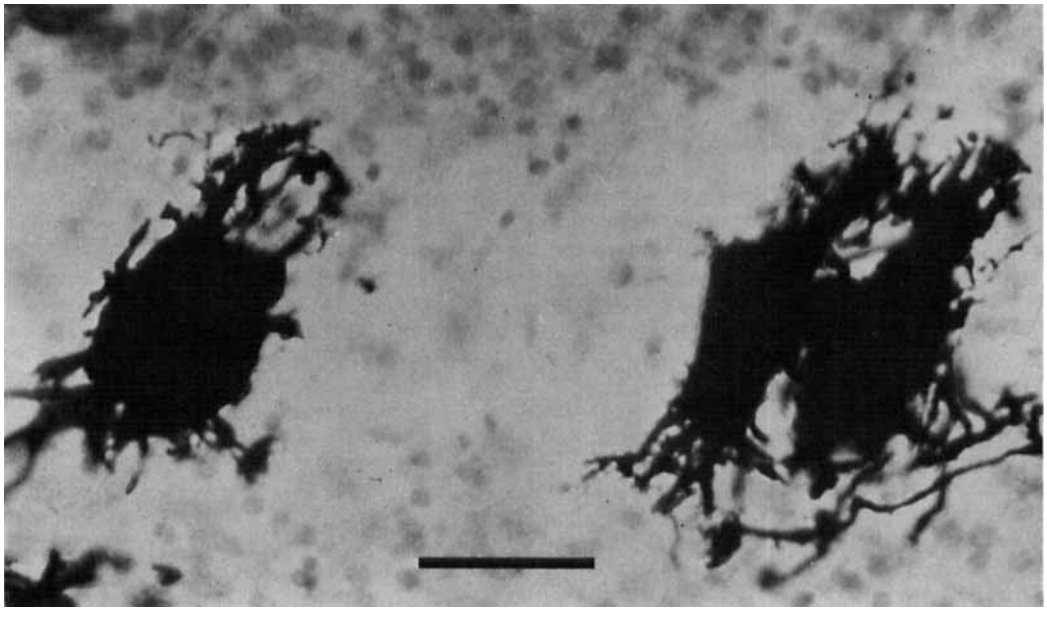

Fig. 1 Golgi-Cox stained sections from the anterior portion of NL, counterstained with cresylviolet. Small glial cell somata can be seen to border the extents of the dorsal and ventral dendritic fields. Four Golgi-impregnated cells are shown. Bar = 50 μm.

methods, which allowed better resolution of fine dendritic morphology than did Golgi-Cox methods. Historically, NL has been found difficult to impregnate with Golgi methods. (Ramón y Cajal, '08; Levi-Montalcini, '49), a problem we have also encountered. It was found, however, that the Stensaas modification of del Rio Hortega's Golgi-Kopsch method is capable of reliably staining a large number of neurons in NL, often offering preparations of great clarity, with the background nearly free of other cells (i.e., glia), provided that the proper time in the fixative is chosen.

The neurons of NL are generally characterized by cylindrical, ellipsoid, or ovoid cell somata, which are spineless and about 20 μm in diameter. The bipolar dendritic trees are generally spineless but rather roughly surfaced and quite frail, with branches averaging about 2 μm in width. Dendrites do not usually issue laterally from the cells, and those that do are generally markedly smaller and thinner. The part of the cell body between the dendritic zones is normally punctuated by a single axon whose initial trajectory is mediad, parallel to the plane of the nucleus, for up to a few hundred micrometers.

The above features of the morphology of laminaris neurons were found to be common to nearly all of the cells in the nucleus. Other features of dendritic morphology, including dendritic size, branching patterns, and the number of dendrites issuing from the cell, change radically across the extent of the nucleus along a gradient from the rostromedial to the caudolateral poles. In each instance the changes are continuously graded across the laminar neurons, and by polythetic criteria these neurons are of a single type (Tyner, '75). The manner of transformation of the cells in the nucleus is best illustrated by the description of a few typical cells taken from different areas of the nucleus.

In the rostromedial third of the nucleus, the cells are largely of the variety seen in figure 2. The cells in this area typically have cylindrical or ellipsoid cell bodies, from which emerge 20 or more short, relatively unbranched dendrites. The dendrites often end in a swelling, sometimes with a bullhorn-like bifurcation of two short processes. While the thickness of the dendrites varies from place to place along their length, there is usually little tapering. Secondary dendritic branches arise from the primary dendrites at practically any point along their length; because of the general shortness of the dendrites it happens that the branching occurs fairly close to the cell soma-

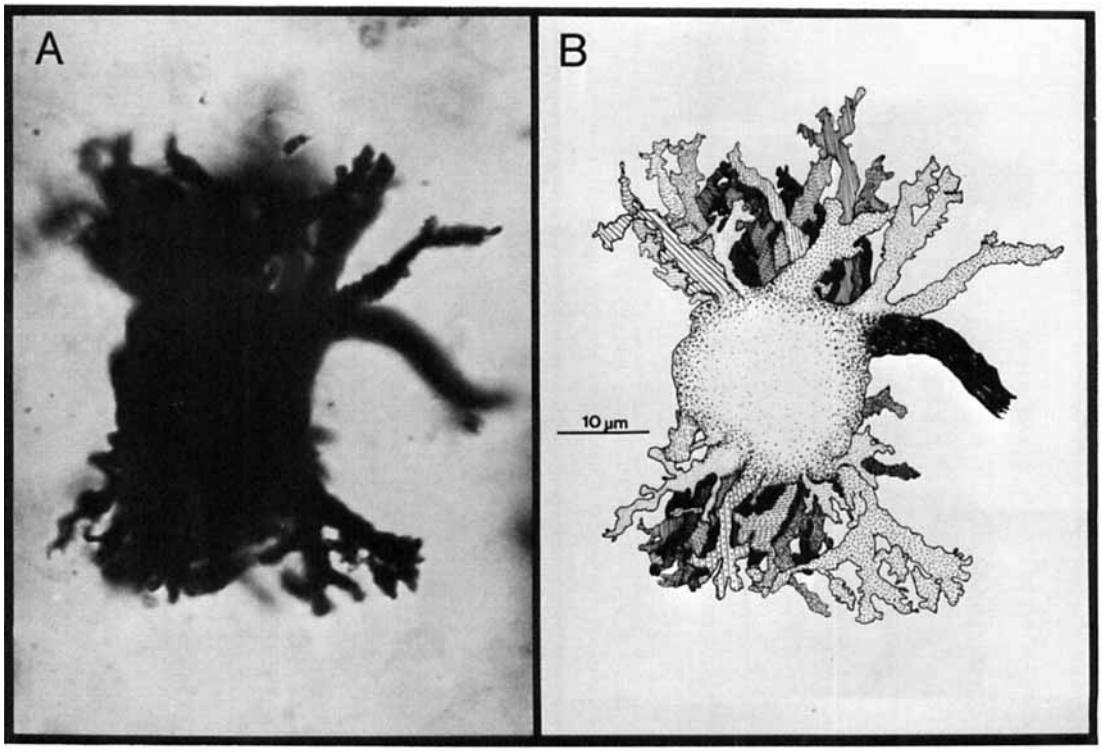

Fig. 2 Cell from the anterior third of NL. Numerous short, rough dendrites issue from the dorsal (top) and ventral sides of the cell. The axon exits from the dorsomedial surface. A. Photomicrograph (n.a. = 1.3) B. Camera lucida drawing (n.a. = 1.3). Golgi-Kopsch method.

ta. Fourth-order or higher-order branches are quite rare.

In the central third of the nucleus, fewer primary dendrites arise from the cell (about 10-15), but these are longer. An example from this area of NL is shown in figure 3. It is not uncommon for the dendrites to issue from either end of the cell in an approximate ring, or for the branching pattern of the dendrites to form a chalice-like arrangement of processes. Dendritic branches of greater than the second order are more common in this area of the nucleus, and there is a tendency for branches to occur at a greater distance from the cell body than is the case more rostromedially. The club-shaped or bullhorn termination of the dendrites is still apparent. The dendritic branches are also longer, and slightly tapered. The cell bodies are usually ellipsoid.

Progressing to the caudolateral third of NL, the interrelated trends of fewer primary dendrites, greater dendritic extension, and more extensive branching at greater distances from the soma are continued (fig. 4), resulting in a neuronal morphology quite different than at the rostromedial end of the nucleus (fig. 5). The cells in this area of the nucleus are characterized by having a few (3-10) relatively stout primary dendrites (2-5 μm wide) which, at the caudolateral pole, progress away from the cell bodies to proliferate eventually into two canopies of very fine fibers oriented parallel to the plane of the nucleus. Third-order and higher-order dendrites are commonly encountered. Very occasionally, a spine-like protrusion or two is seen on the primary dendrites. In the extreme caudolateral pole of the nucleus, very thin spiny dendrites are seen in the dendrite canopies, but it has not been possible to trace them to cells of origin in NL. The gradient of transformation of structure in NL is illustrated in figure 6, which shows cells from a single coronal section through NL.

Occasionally, a few neurons with different morphologies than those described above are seen in, or close to, the laminar nucleus. On the basis of position and morphology, these

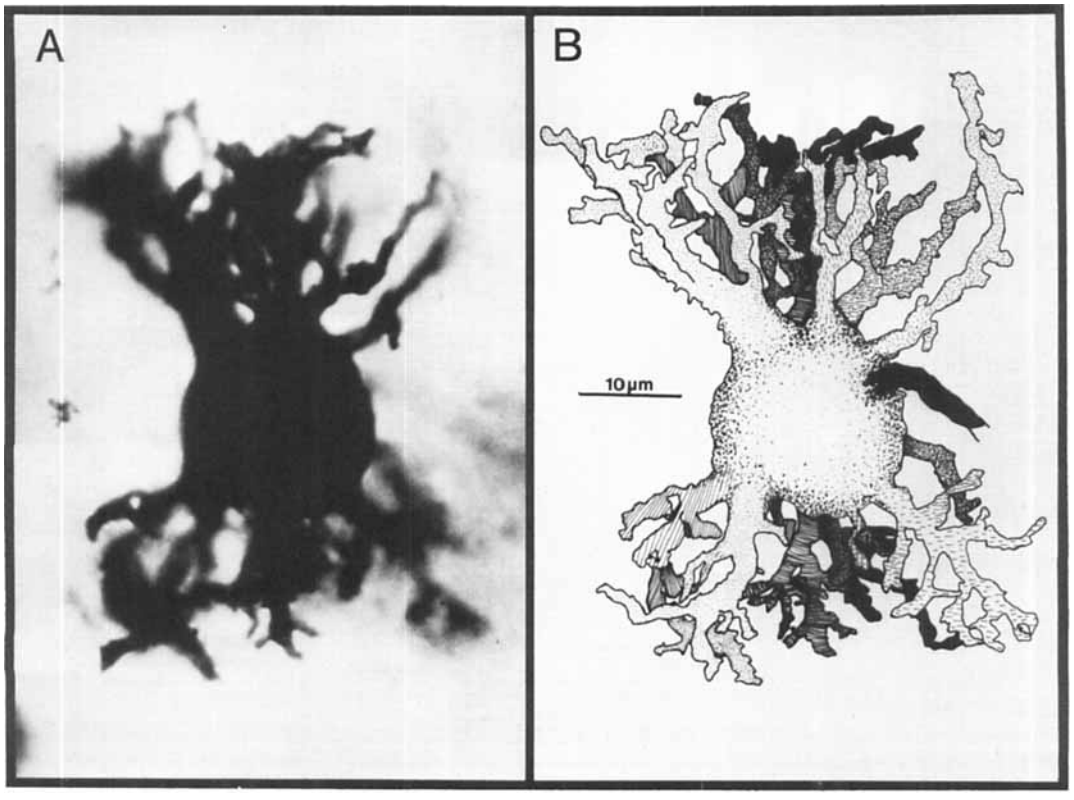

Fig. 3 NL cell located approximately one-third the distance from the anterior to the posterior poles of the nucleus. Compared to cells located more rostrad in NL (cf. fig. 2) there are fewer primary dendrites, which branch more and have a greater extension. A. Photomicrograph (n.a. = 1.3). B. Camera lucida drawing (n.a. = 1.3). Golgi-Kopsch method.

cells have been assigned to two groups. The cell bodies of the first group, the perilaminar neurons, are found just dorsad to the line of NL cell bodies. They are of approximately the same size as the somata of the laminar neurons, and the dendrites are of similar caliber and morphological details as the subjacent cells of n. laminaris (fig. 7). The four to eight primary dendrites of these cells are not arranged in a bipolar fashion, however. They pour ventrad out of the soma toward the laminar nucleus and into the surrounding fibers, often branching to form a cone of processes, resembling a drapery. The dendrites do not quite reach those of the laminar neurons. No systematic variation of dendritic length, number, or branching with the position of these cells has been noted. The initial axon segment leaves the cell from the dorsal surface, but its final destination is moot: the cells are not labeled after HRP injections into the cochlea (Parks and Rubel, '78). Thus they are probably not the origin of cochlear efferents. These perilaminar cells appear to exist in the ratio of about 3 for every 100 laminar cells; their comparative rarity has been verified by observations of Nissl-stained sections, where they are detectable by their size and position. Because of the similarities in soma size and dendritic morphology between these perilaminar cells and the laminar neurons it is possible that they are ectopic laminar cells; for the purposes of analysis of the dendrites in NL, however, they have been classed separately.

Another group of cells seen in NL is even less frequently encountered, less than 1 per 100 laminar neurons, and has a morphology most unlike other laminaris cells (fig. 8). These cells have a few large (3-5 μm in diameter) spine-studded dendrites which emerge from a spiny soma of greater size than of the laminar neurons. Despite their comparatively greater width, the dendrites of these cells are rather short, often oriented in the plane of the

nucleus, but sometimes outside of it. These cells may be found in any portion of the nucleus, though the cell body is commonly found with those of the laminar cells. The axon may leave the cell in any direction, for an unknown destination. These cells were not included in the quantitative analyses of NL which follow.

Quantitative analyses

Measurement validation

Accuracy of the drawings and of the planimetry was determined by repeated drawings and measurements. For the areal drawings and measurements, the errors of drawing and of measurement were less than 1% (0.98% and 0.2% , respectively). For the length drawings and measurements the error of drawing was less than 1.1%, and the error of measurement was under 3.0%. Since these drawings were made at three different final magnifications, the error introduced by this variation was assessed, and found to be under 2.4%. These error values were deemed sufficiently small to allow confidence in the accuracy of analyses and predictions based upon these data; and since no consistent bias could be found, the data were left uncorrected.

The positions of the cells sampled for quantitation, as determined from the Golgi sections, were plotted on the mean planar projection of NL from Nissl sections, and are shown in figure 9. In general, it can be seen that the fit is quite good. Some cells, however, lie somewhat lateral to the extent of the mean planar projection of the nucleus. There are two likely causes for this. The first is the inaccuracy introduced by the Golgi sections in our ability to determine precisely the lateral margin of the nucleus. The second explanation is variation in sectioning angle. Nearly all of the cells more than one standard deviation outside of the planar projection are from a single animal, and such a distribution has been seen in Nissl-stained brains when the section angle is somewhat askew. Despite these minor difficulties, the distribution of the sampled cells from the Golgi sections corresponds closely to the independently-acquired measure of the distribution of the nucleus given by the mean planar projection from Nissl-stained material.

The relationship between dendritic length and dendritic area was examined by measurements of both parameters from nine cells taken from different parts of the nucleus (positions shaded in black in fig. 9). Independent measurements were made of the longitudinal

Fig. 4 Photomicrograph of a pair of cells in the posterior third of NL, showing a continuation of the trends of fewer, longer, and more branched dendrites. Rapid Golgi method. Bar = 50 μm.

area of the dorsal dendrites, and of the ventral dendrites, from area drawings exemplified in figure 10B. Corresponding measurements of the dorsal and ventral lengths were taken from the drawings for length measurement of the cells, as shown in figure 10C. The correspondence of the dorsal and ventral areas with the lengths is shown in figure 11. The two measures were found to be highly correlated ($r = 0.96$, $p < 0.001$), indicating that measures of dendritic length are also valid estimators of dendritic area. This conclusion, it should be noted, is valid throughout the nucleus, regardless of the length measured. It is a reasonable surmise, though not directly tested in this study, that the dendritic area measured is highly correlated with dendritic surface area. Therefore, measurements of dendritic length may be extrapolated to indicate dendritic surface area, or dendritic size, in general.

Total dendritic length

The total dendritic length is the sum of the lengths of the dorsal and ventral dendritic processes of a neuron. In order to determine if dendritic size varied systematically across the

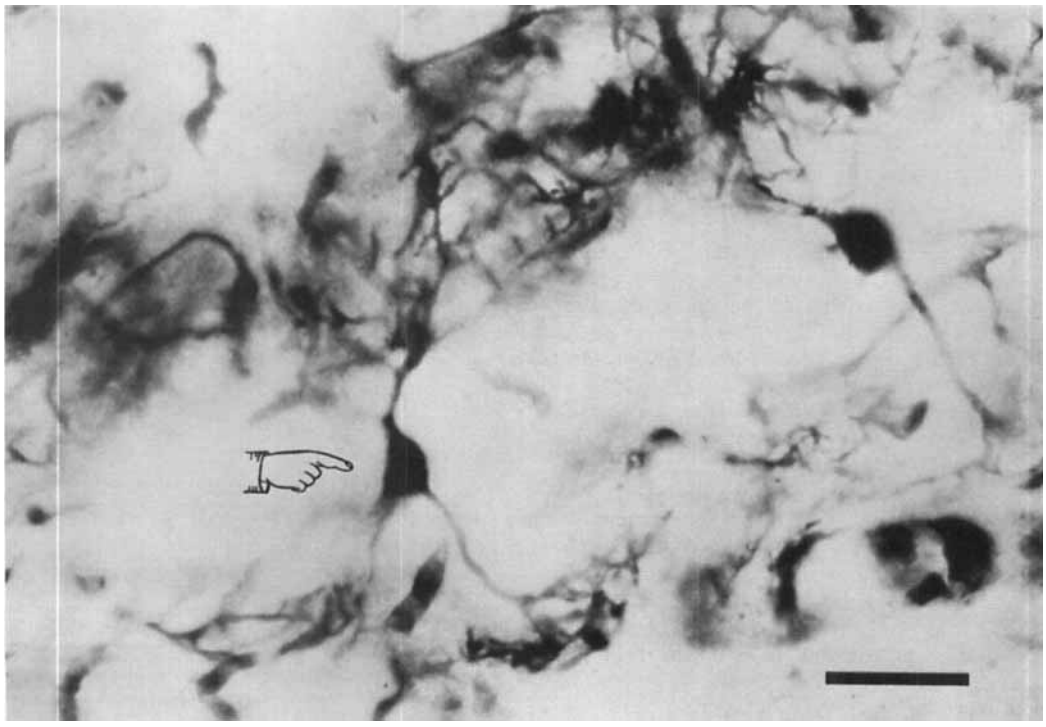

Fig. 5 Low-power photomicrograph of cells at the caudolateral pole of NL. The dendritic branches form a canopy of processes dorsal (top) and ventral to the plane of cell bodies, which is indicated by the clear zone in which two cell somata may be seen. A camera lucida drawing of the cell at left center (pointer) is shown in figure 10A. Golgi-Kopsch method. Bar = 50 μm.

two dimensions of the nucleus, this parameter was related to the two orthogonal positional variables of the measured cells.

As indicated in figures 12A,B there is an orderly and continuous increase in the total dendritic length of neurons as one traverses the nucleus from anterior to posterior or from medial to lateral. The regression of total length on position posterior-to-anterior is highly significant ($r = -0.59$, $p < 0.0001$).[2] Thus the rostrocaudal position of neurons in NL accounts for about 35% of the variance in dendritic length. The regression of total length on the lateral-to-medial dimension was similar ($r = -0.57$), accounting for about 33% of the variance. Since dendritic size correlates with both dimensions of NL the overall best prediction of the changes in total length with neuronal position may be obtained with a multiple regression of total length on the P-A and L-M positions. The results of this analysis are seen in figure 12C. As expected, when both dimensions are taken into account, the ability to predict the total dendritic length from the position in the nucleus is improved ($r = -0.70$); altogether, 50% of the variance of the total length may be accounted for by position within the nucleus. As indicated by the similarity of the multiple regression coefficients, the contributions of the P-A and L-M dimensions to the gradient of the total dendritic

[2] Unless specified otherwise, all correlations and regressions are significant at this level.

Fig. 6 (Top) Camera lucida drawing of nucleus magnocellularis (NM) and nucleus laminaris (NL) from a coronal section about three quarters of the anterior-to-posterior extent of the nucleus. The change in dendritic morphology in NL from medial (left) to lateral (right) is apparent. No such change is seen in NM. Another, rare type of neuron found in NL is indicated at "A" (cf. fig. 8). Golgi-Kopsch method. (n.a. = 1.3).

(Box) Composite drawing showing the manner in which the afferents from NM distribute across NL. The afferents from the ipsilateral NM (pointer) branch a number of times in their approach to NL (most branches not drawn). The ventral afferents send collateral branches to the NL neuropil. Arrow points dorsad. Cross bar = 100 μm for the top drawing and 75 μm in the lower.

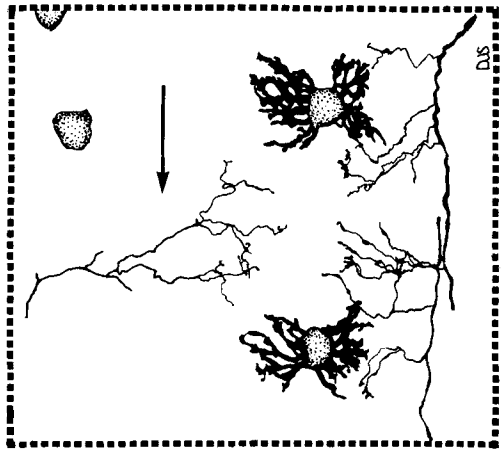

Figure 6

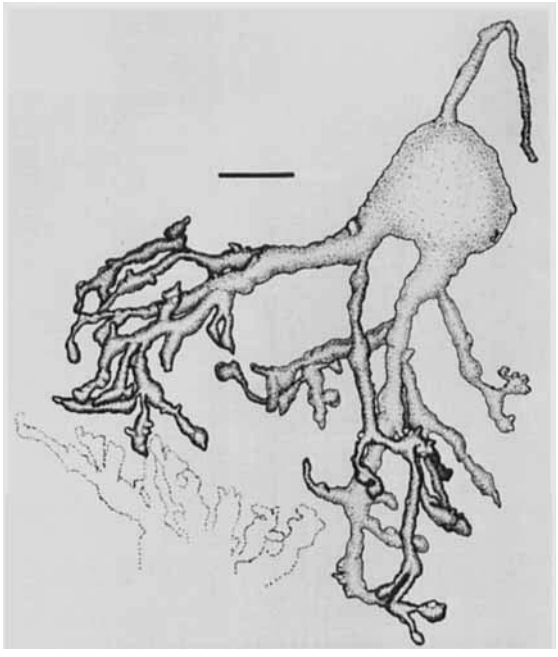

Fig. 7 Camera lucida drawing of a perilaminar cell located just dorsal to the plane of NL cells. The dendrites of a nearby NL neuron are outlined in dots, below. (n.a. = 1.3) Bar = 10 μm.

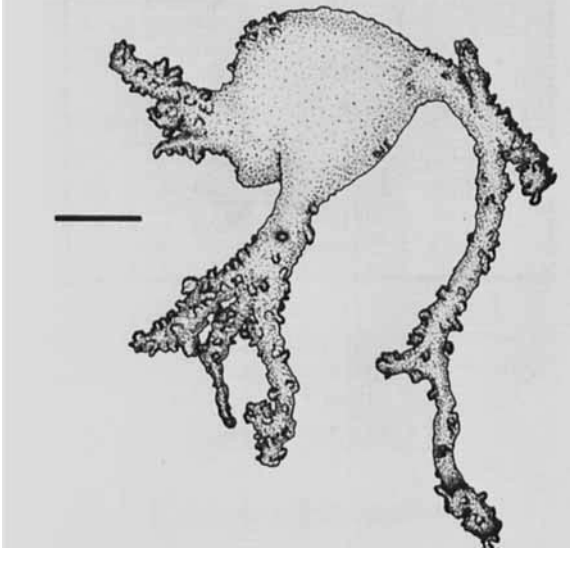

Fig. 8 Camera lucida drawings of a spiny-type neuron, occasionally encountered in NL. (n.a. = 1.3) Bar = 10 μm.

length in the nucleus are roughly equal. This can be seen in figure 12D, which shows the gradient of dendritic length increase plotted across the planar projection of NL.

Number of primary dendrites

Closely paralleling the gradient of increasing dendritic size there is a rostromedial-to-caudolateral gradient of decrease in the total number of primary dendrites issued from the cell bodies, from an average of 32 down to 3. Figure 13A shows the results of the regression of the total number of primary dendrites on the P-A dimension ($r = 0.63$), and the same analysis for the L-M dimension is shown in figure 13B ($r = 0.69$). It should be noted that in both these figures the floor to the regression function has been drawn at three dendrites, the minimal number that was observed for any cell. This same proviso applies to figure 13C, which shows the result of the multiple linear regression of the number of primary dendrites on position P-A and L-M ($r = 0.81$). Figure 13D shows the resulting gradient of increase in the number of primary dendrites across NL. Except for the reversed caudorostral polarity, it is identical to the gradient of total length described for the nucleus (cf. fig. 12). The inverse relationship found between dendritic length and the number of primary dendrites is reminiscent of a similar inverse relationship between branching complexity and dendrite number in the rat and cat cortex (Samuels et al., '77).

Relationship of dendritic length and number to frequency organization

As we have previously described (Rubel and Parks, '75), NL is organized tonotopically, with cells having high characteristic frequencies (~4,000 Hz) found at the rostromedial pole of the nucleus, and cells with progressively lower characteristic frequencies found progressively caudolaterad. This tonotopic organization results from a discretely organized projection to NL from the two magnocellular nuclei (Parks and Rubel, '75). The relationship of the dendritic parameters discussed above to this frequency gradient in NL was next examined.

By determination of the position on the planar projection of the units whose characteristic frequencies (CF's) were determined, Rubel and Parks ('75) were able to quantitatively describe the gradient of frequency

across NL on the basis of the rostrocaudal and mediolateral positions (frequency (kHz) = 0.027 (%P-A) + 0.014 (%L-M) − 0.88; r = 0.94). In order to compare directly the gradients for frequency, length, and dendritic number, which are in different units, it was necessary to convert the data to standard units (z-scores), which may be directly compared without in any way altering the regression functions found. (Because the polarity of the gradient of dendritic length is opposite to that of frequency and number, the negative z-scores for length were taken.) The results of the normalized regression functions for total length, total number of primary dendrites, and for characteristic frequency on position are shown in figure 14A. As can be seen, the gradients for frequency, dendritic length, and dendritic number across NL are essentially identical.

In figure 14B this information is summarized by showing the NL planar projection as a slice whose thickness is proportional to total dendritic length.

Comparison of dorsal and ventral dendritic lengths

The close relationship between the total length of dendrites and frequency in this nucleus implies there is a correlation between the frequency organization of NL and the total dendritic surface area. Since the tonotopic organization of NL results from spatially segregated afferent projections from each magnocellular nucleus, we next investigated the correspondence between the size of the dorsal and the ventral dendrites of NL cells on a cell-by-cell basis and in relation to the frequency organization of the nucleus.

The relationship between the dorsal and ventral dendritic lengths, when taken on a cell-by-cell basis, is shown in figure 15. The correlation, though highly significant ($r = 0.47$, $p < 0.001$), is not particularly close, as evidenced by the amount of scatter on the plot. Though cells in NL receive similar information from the two ears (as evidenced by similar characteristic frequencies and thresholds to sound stimulation of either ear (Rubel and Parks, '75)), the comparative weakness of the correspondence between the dorsal and ventral dendritic lengths indicates that, for any single cell, there can be fairly large differences in the amount of dendritic area offered to the two sets of afferents from NM.

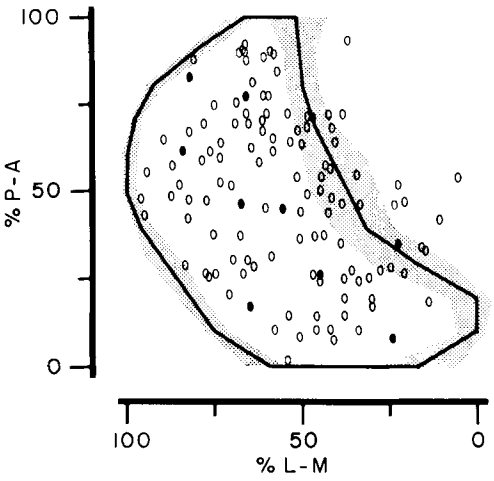

Fig. 9 Mean planar projection of NL on the right side of the brain, as constructed from Nissl-stained sections (METHODS). Shaded zones indicate ± 1 standard deviation from the mean planar projection. Ellipses indicate the positions of the cells used in the quantitative analyses, as determined from the Golgi sections. Filled ellipses denote the positions of the cells used to correlate dendritic length with cross-sectional area (fig. 11). Each ellipse subtends 2% by 3% of the dimensions of the planar projection, which corresponds to the area in NL subtended by the average cell soma of 20 μm diameter.

The distribution of afferents to NL from NM is not, however, to individual cells in NL, but rather these afferents can be seen to distribute themselves across a group of cells within an isofrequency band, as observed by injection of single cells in NM with horseradish peroxidase (Jackson et al., '78), or by Golgi methods (Cajal, '08; Jhaveri, '78). This suggests that rather than considering the relationship of the dorsal with the ventral dendritic size on a cell-by-cell basis, it would be more efficacious to analyze it on an area-by-area basis, taking the characteristic frequency organization into account. To this end, NL was divided into eight sectors orthogonal to the frequency gradient (as defined from Rubel and Parks, '75), so that all the cells within a sector may be expected to have CF's within 500 Hz of each other, as shown in figure 16A. For the 10 to 24 cells sampled within each sector, the mean dorsal and mean ventral dendritic lengths were calculated, and these were then correlated with each other across sectors. The result of this correlation is shown in figure 16B. The correlation is excellent ($r = 0.93$, $p < 0.001$). Thus, when averaged within

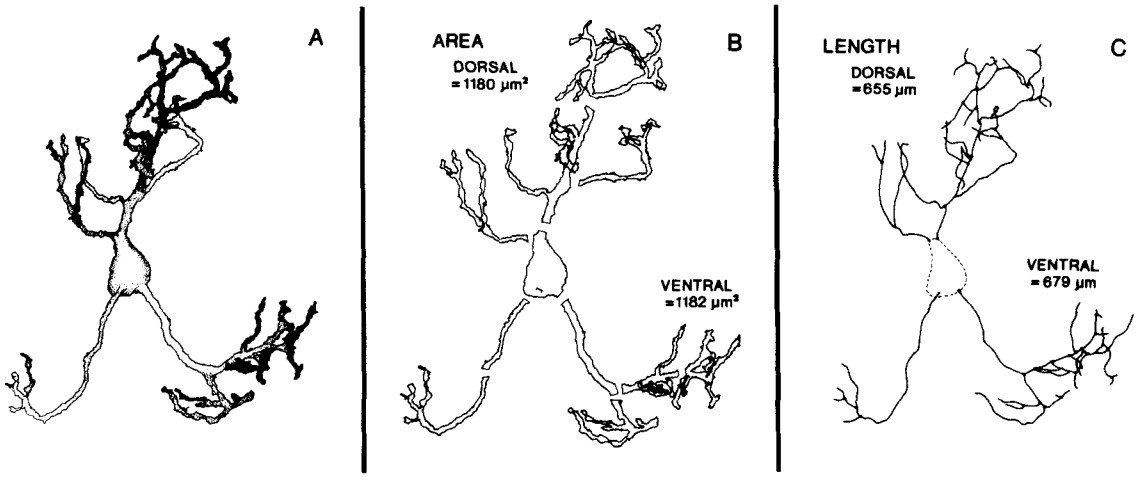

Fig. 10 Three views of the neuron seen in figure 5, to illustrate the methods of drawing for quantification. A. Camera lucida drawing of the cell. (n.a. = 1.3) B. Camera lucida drawing of the cell in outline, of the type used to measure dendritic longitudinal area. To insure equal magnification of the field of view, the dendritic arborizations were drawn in sections, as shown. (100 × oil immersion objective, n.a. = 1.3; achromatic aplanatic condenser, n.a. = 1.4) C. Camera lucida drawing of the type used to measure dendritic length. In these drawings dendritic processes were represented by lines traced down their middles. (n.a. = 1.3 or 1.4; condenser, n.a. = 1.4).

TABLE 1

Dorsal and ventral dendritic lengths analyzed within the isofrequency sectors shown in figure 16A

Sector	Number of cells	Mean	s.d.	r[1]	p
1 dorsal	10	356.2	81.03	0.16	n.s.
ventral		245.0	77.92		
2 dorsal	12	371.6	129.21	0.26	n.s.
ventral		295.4	106.05		
3 dorsal	24	343.9	101.42	0.46	<0.05
ventral		315.3	87.84		
4 dorsal	15	437.2	127.96	0.22	n.s.
ventral		353.6	93.11		
5 dorsal	24	460.9	143.77	0.35	n.s.
ventral		461.4	142.41		
6 dorsal	15	515.5	148.35	0.34	n.s.
ventral		533.9	179.57		
7 dorsal	15	588.3	162.22	0.08	n.s.
ventral		509.2	181.23		
8 dorsal	10	579.4	128.61	−0.25	n.s.
ventral		558.7	161.66		

[1] r, product-moment correlation of dorsal and ventral dendritic lengths within designated sectors.

an isofrequency zone in NL, the amount of dorsal dendritic area available for afferents from the ipsilateral NM is closely tied to the amount of the ventral dendritic area available to the terminals from the contralateral NM; this is so even though the correlations of the dorsal and ventral dendritic lengths on a cell-by-cell basis within each isofrequency band are not high (table 1). This result moreover is not simply an artifact of averaging the dorsal and ventral lengths within arbitrary sectors, for the correlations of the mean dorsal with mean ventral dendritic lengths when taken across sectors other than the isofrequency zones were not statistically significant, and not significantly improved over those of the individual cells alone (for 8 sectors at 45° to the isofrequency bands, r = 0.63; for 8 sectors

at 90° angles to the isofrequency bands, r = −0.27).

Dorsal and ventral gradients of length and number

The above finding that there is a gradient of total length across the nucleus strongly implies that such a gradient for the dorsal and ventral lengths taken independently also exists. However, the dorsal and ventral dendrites are segregated in this nucleus, and moreover, the inputs to the two dendritic fields are also strictly segregated (Boord, '68; Parks and Rubel, '75). Thus, the possibility exists that the morphology of the dorsal and ventral dendrites to some degree may be regulated independently. This was assessed by separate regression analyses of the dorsal and ventral dendrites as a function of neuronal position, as shown in figure 17. For the dorsal dendritic length, regression on the P-A dimension alone shows a stronger relationship than on the L-M dimension alone (dorsal length on P-A, r = −0.53; dorsal length on L-M, r = −0.36). The difference between these two regressions for dorsal length is significant ($p < 0.05$). For ventral dendritic length the situation is reversed: a stronger relationship holds with the L-M dimension than with the P-A dimension (ventral length on P-A, r = −0.49; ventral length on L-M, r = −0.60). These two regressions of ventral length on position are also significantly different ($p < 0.05$).

To determine the overall gradients of dorsal and ventral length across the nucleus, independent multiple linear regressions of dorsal length on position and of ventral length on position were performed. The multiple regression of dorsal length on position P-A and L-M is shown in figure 18A (r = −0.56). It is also apparent from the absolute size of the regression coefficients for the positional variables that the contribution of the P-A dimension to the gradient of dorsal dendritic length is greater than that of the L-M dimension (−3.12 for P-A vs. −1.56 for L-M). For the ventral dendritic length, the result of the multiple regression is shown in figure 18B (r = −0.68) and, in contrast to the dorsal dendrites, in the case of the ventral dendrites' length the L-M dimension is the major contributor to the gradient (−2.37 for P-A vs. −4.12 for L-M). The two gradients, for dorsal and for ventral dendritic length, are plotted on the planar projection of NL in figure 18C.

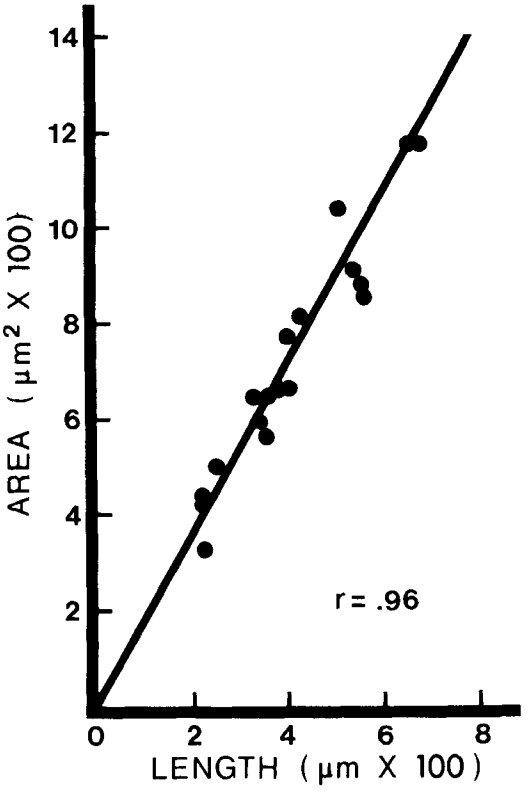

Fig. 11 Scattergram and least-squares fit line relating dendritic longitudinal area with dendritic length. The correlation of these two measures is shown. The high correlation of the two variables indicates measures of dendritic length are proportional to dendritic area. Measures were correlated from the dorsal and ventral dendrites of nine cells (filled positions in fig. 9). (n = 18; slope of line = 1.78).

Thus the length gradient for the dorsal dendrites is predominantly along the rostrocaudal axis, while that of the ventral dendrites is dominated by the contribution of the mediolateral axis. These data indicate that there is a measure of separate regulation of dendritic lengths in the two dendritic fields of NL.

Such a separate regulation of the dorsal and ventral dendritic length gradients is not inconsistent with the aforementioned finding that the dorsal and ventral dendritic sizes are closely related within isofrequency bands. This is because the dorsal and ventral length gradients are skewed equally to either size of the frequency gradient (or length gradient, figs. 12, 14). A consequence of this symmetrical skewing is that the average dorsal and ventral dendritic sizes within isofrequency

zones are closely related. If either the dorsal or ventral size gradients were skewed farther from the frequency gradient than the other, the close correspondence between dorsal and ventral dendritic sizes within the isofrequency zones would not be possible.

Since the dorsal and ventral lengths are regulated somewhat independently, as evidenced by their separate gradients across the nucleus, it might be expected that similar analyses of dorsal and ventral dendritic number would reveal evidence of separate regulation. The results of the separate multiple linear regression analyses of dorsal dendritic number and ventral dendritic number on position are shown in figure 19A and B ($r = 0.74$ in both cases). As shown in figure 19C, there is again evidence for two gradients across NL, one for the number of primary dorsal dendrites and another for ventral dendrites. These two gradients are not quite as divergent as those seen for the dorsal and ventral length, which is also reflected in the finding that the correlation between the number of dorsal primary dendrites and the number of ventral primary dendrites ($r = 0.66$) is somewhat higher than that for length.

The relationship of dendritic length to soma size

For 51 cells sampled throughout the nucleus, measures of the area of the somata were taken. The mean area of the somata in NL is 306 μm^2 (SD = 67.9). There is a weak correlation of cell soma size and position of the cell in NL ($r = 0.36$, $p = 0.03$), though for the most part soma size in the nucleus is rather constant throughout. Examination of this datum revealed the above correlation to result from a small number of somewhat larger cells at the caudal end of NL. However, neither the correlation between cell body size and the total length of dendrites issued by the cell ($r = 0.13$), nor between the cell size and the number of dendrites ($r = 0.26$) was statistically significant. These findings negate the possibility that the gradients of dendritic size or number are the result of a gradient of soma size, or that soma size and dendritic size or dendrite number are at all closely related in this nucleus. This result was somewhat unexpected in view of the 3-fold increase in dendritic size across NL (Hinds and McNelly, '77; but see Mannen, '66; Gelfan, '70; and Berry et al., '72).

DISCUSSION

Of greatest interest, within the context of our research program (see Rubel, '78; Rubel et al., '79), are the findings of predictable and orderly relationships of dendritic organization within NL. While the significance for auditory functioning of the correlation of dendritic structure with the tonotopic map of NL is yet unknown, the nature of the morphological gradients does possess implications for neuronal development. Before discussion of this point, however, some consideration of the quantification procedures employed, and of the relationships of dendritic structure of NL with that of its possible mammalian homologue, is in order.

Quantification of dendritic parameters

Most previous measures of dendritic field size have employed the concentric-circle analysis of Sholl ('53) or the target modification of Eayrs ('55). Measurement of dendritic parameters based on this procedure have been criticized due to their large projection error, especially in neurons with extensive domains in all three dimensions (Berry et al., '72). In certain instances, however, it is appropriate to employ measurements of dendritic parameters from camera lucida projections. These occur when all of the processes of the measured neuron are contained in the same section and when the extent of the dendritic processes in the third dimension is minimal. Cell types which have permitted such techniques of measurement include the cerebellar Purkinje cell (Bradley and Berry, '76; Berry and Bradley, '76a,b; McConnell and Berry, '78a,b) and the stellate cell of the visual cortex (Eayrs and Goodhead, '59; Borges and Berry, '76, '78). The cells of NL are also amenable to study by camera lucida drawings. The bipolar origin of the dendrites allows the cells to be completely contained in either coronal or sagittal sections, and nearly eliminates effects due to shadowing by the cell body, as dendrites only rarely issue from the sides of the cells.

The dendrites of NL cells are not, however, perfectly flat. While the data presented in figure 11 argue that the linear measurements are directly proportional to their absolute cross-sectional areas, these nonetheless must be somewhat underestimated because of errors resulting from the 2-dimensional projection. Because of the number of dendrites mea-

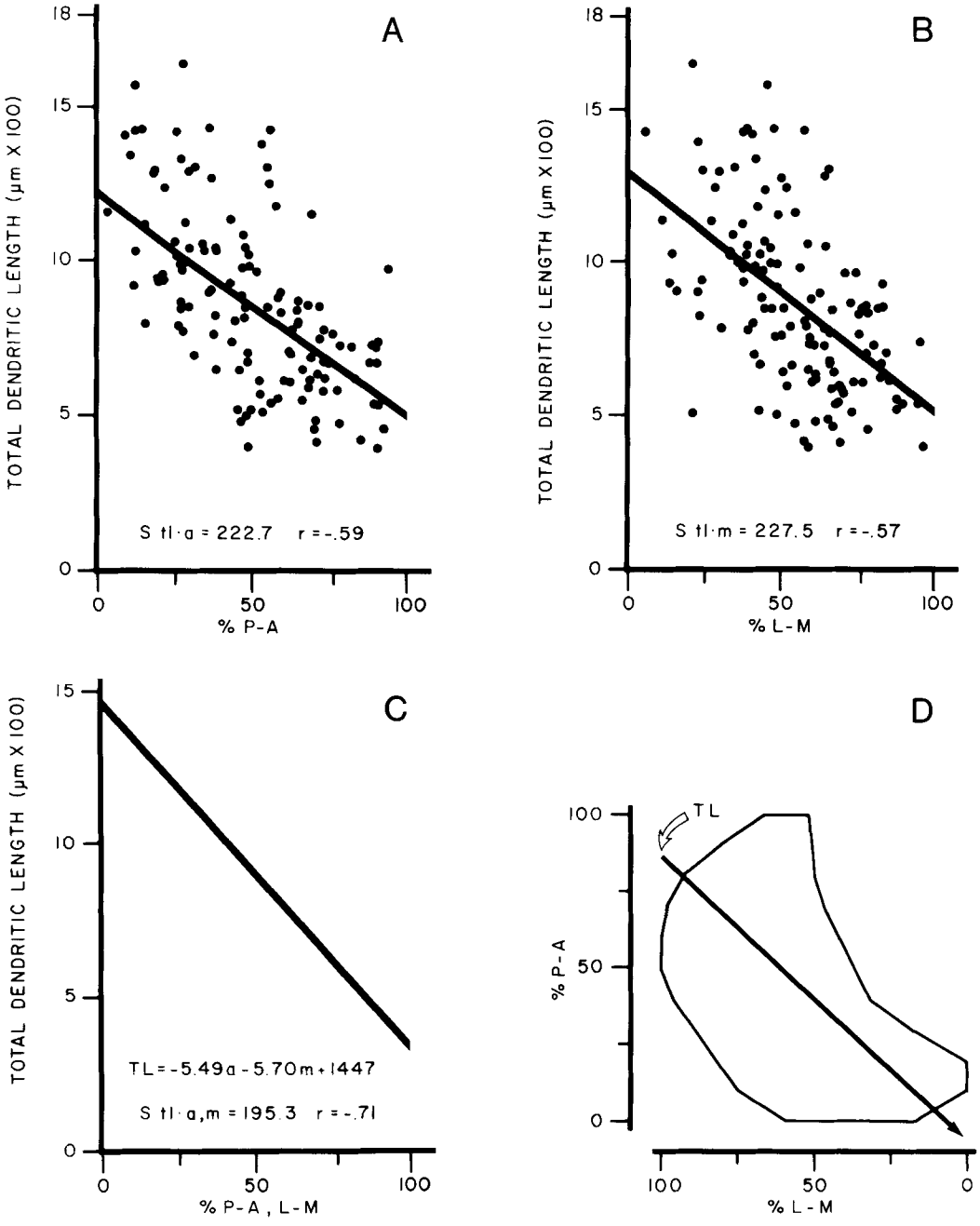

Fig. 12 The relation of total dendritic length of NL neurons to their positions within the nucleus. A. Scattergram and regression relating total dendritic length to position along the posterior-to-anterior dimension of NL. The standard error of estimate and correlation coefficient are shown. (n = 127; regression equation for total length = −7.18 (%P-A) + 1222). B. Scattergram and regression relating total dendritic length to position along the lateral-to-medial axis. The standard error of estimate and correlation coefficient are shown. (n = 127; regression equation for total length = −7.77 (%L-M) + 1282). C. Multiple regression relating total dendritic length to both the posterior-to-anterior and lateral-to-medial dimensions of NL. The regression equation, standard error of estimate, and correlation coefficient are shown. (n = 127). D. The gradient of increase of total dendritic length plotted across the planar projection of NL. The gradient of total dendritic length is defined as a line orthogonal to the isopleths for total length, as derived from the multiple regression equation (cf. fig. 16A). TL, total dendritic length.

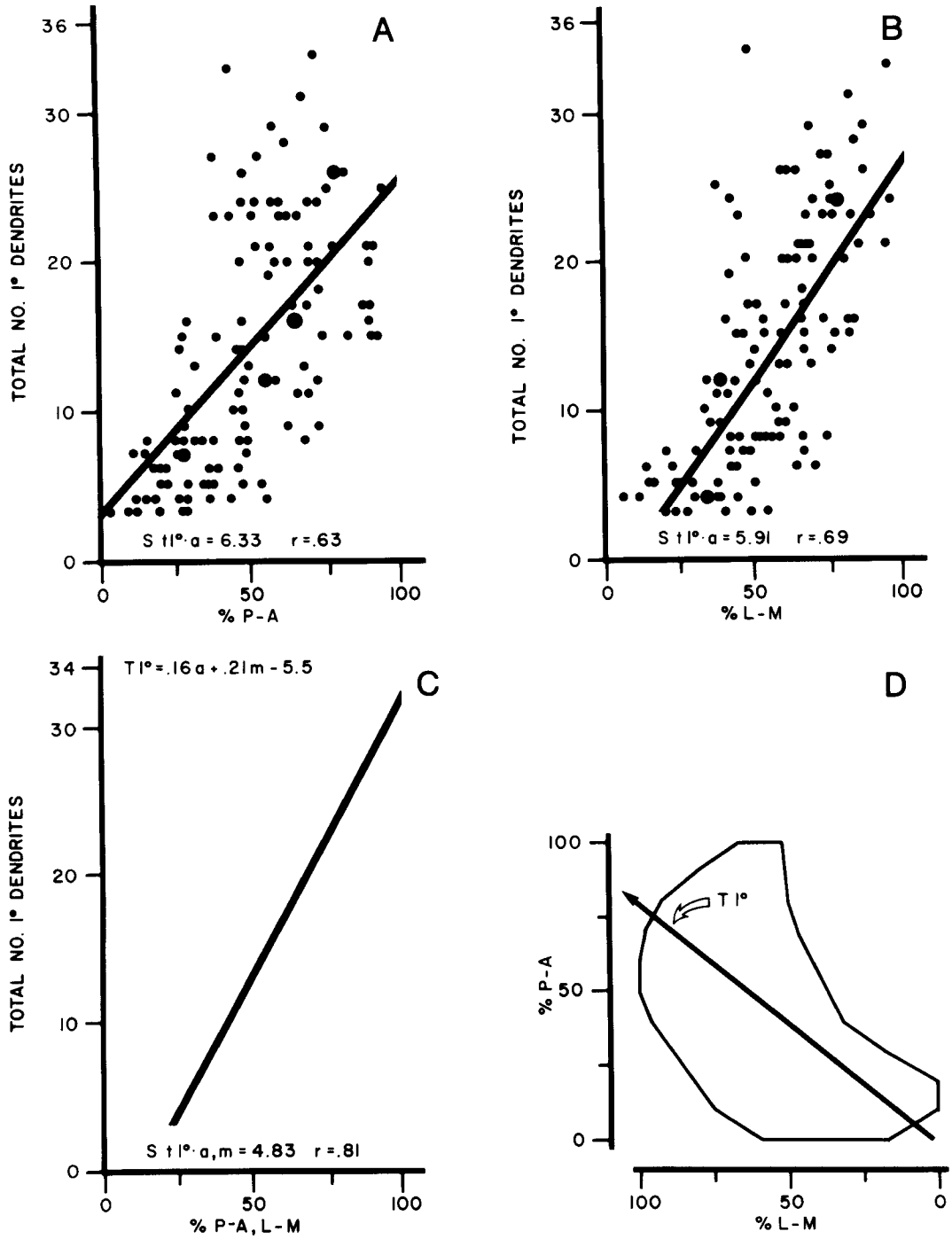

Fig. 13 The relation of the total number of primary dendrites of NL neurons to their position within the nucleus. A. Scattergram and regression relating the total number of primary dendrites with position in the posterior-to-anterior dimension of NL. The standard error of estimate and correlation coefficient are shown. The data and the regression line in this figure have a floor at 3 dendrites, the fewest observed for any NL cell. (n = 122; regression equation for total number of dendrites = 0.227 (%P-A) + 2.82). B. Scattergram and regression relating total number of primary dendrites to position on the lateral-to-medial axis of NL. The standard error of estimate and correlation coefficient are shown. (n = 122; regression equation for total primary dendrites = 0.274 (%L-M) −0.745). C. Multiple regression relating the total number of primary dendrites to both positional variables. The regression equation, standard error of estimate, and correlation coefficient are shown. (n = 122) D. The gradient of increase in the number of primary dendrites of NL cells plotted across the planar projection of the nucleus. For the derivation of the gradient, see figure 12. The gradients of total dendrite number and total dendritic length are nearly identical, though of opposite polarity (cf. fig. 12D). T 1°, Total number of primary dendrites.

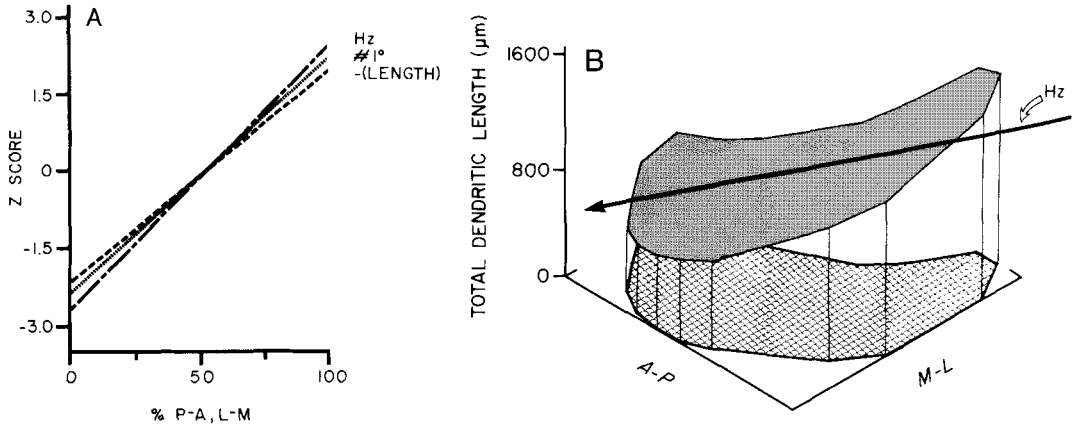

Fig. 14 The relationship of the gradients for predicting characteristic frequency, dendrite number and dendritic length in NL. A. Multiple linear regressions relating the characteristic frequency (Hz), total number of primary dendrites (#1°), and total dendritic length (length) of NL neurons with their position in the posterior-to-anterior and lateral-to-medial dimensions of the nucleus. For comparison, the data for the dependent variables have been normalized (converted to z-scores); because of the opposite polarity of the length gradient, the negative values of its z-scores have been plotted (see text for details). It can be seen that all three gradients across NL are nearly identical. B. Isometric view of the planar projection of NL (lower surface, pincushioned) with the regression plane of total dendritic length (grey surface) plotted above it. On the dendritic length regression plane is shown the gradient of increasing characteristic frequency of NL cells (Hz). Data pertaining to the frequency organization of NL from Rubel and Parks ('75).

sured in this study (about 1,800) and the difficulty in making accurate 3-dimensional measures of length (Gelfan et al., '70), no attempt was made to compensate for foreshortening of dendrites due to projection. Fortunately, in NL the dendrites do not usually deviate more than 45° from the coronal plane of section (as seen in sagittal sections), so the overall correction factor (Bok, '59) for the absolute length is probably less than 1.4 anywhere in NL. Thus, the absolute error is doubtless proportional to dendritic length, and is largest where the dendrites are longest. Finally, a previous study which examined the correlation between the 2-dimensional projected lengths of pyramidal cell dendrites and measurements taken in three dimensions revealed them to be highly correlated (Coleman and Riesen, '68). It is therefore highly unlikely that any of the gradients observed could have resulted from measurement artifact. The actual lengths of NL dendrites and possibly the numbers of dendrites may be slightly higher than indicated in this study because of technical limitations. These factors, however, do not affect the measurements of the relative changes, or gradients, of dendritic length and number across the nucleus.

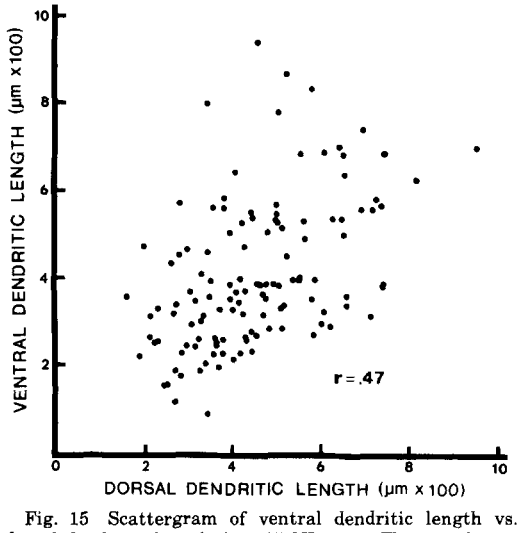

Fig. 15 Scattergram of ventral dendritic length vs. dorsal dendritic length for 125 NL cells. The correlation coefficient is shown.

Comparison with previous descriptions of NL and with the mammalian medial superior olive

The most complete descriptions of the dendritic structure of NL prior to this study are

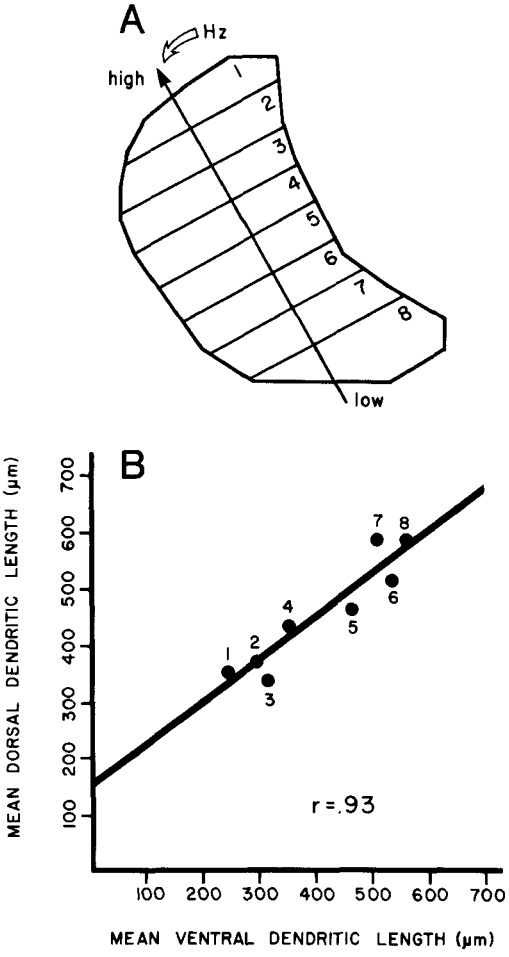

Fig. 16 The relationship of average dorsal and average ventral dendritic lengths when considered across isofrequency zones. A. Planar projection of NL on which has been plotted the gradient of characteristic frequency (Hz) across the nucleus. NL has been divided into 8 sectors by 7 isopleths for frequency at intervals of ~400 Hz (data from Rubel and Parks, '75). B. The mean dorsal dendritic lengths plotted against the mean ventral dendritic lengths of the 10-24 cells in each of the sectors shown in A. The correlation coefficient and least-squares fit line are shown.

brief sections in the work of Ramón y Cajal ('08, '71). The variation in dendritic morphology across NL was also apparent to him (Ramón y Cajal, '08: p. 201). Ramón y Cajal's descriptive studies of this nucleus were based on rapid Golgi impregnations of chick and sparrow embryos at 15-17 days of incubation; he reported that the Golgi technique succeeded for him only with a few embryos. Cajal's use of embryonic tissue, as compared with our use of posthatch material, may explain the discrepancy between his descriptions of the cells as fusiform with spiny dendrites and our description of spineless (though not smooth) dendrites and generally ovoid cell somata. The case here may be similar to that of the mammalian medial superior olive (MSO), where Cajal's observations of fusiform bipolar cells with spiny dendrites (Ramón y Cajal, '71) have not been confirmed in older cats, which appear to have MSO neurons with smooth or moniliform dendrites, while dendritic spines appear to be characteristic of MSO neurons in young animals (Scheibel and Scheibel, '74; Schwartz, '77). On the other hand, preliminary analysis of embryonic NL cells impregnated with the Golgi-Kopsch method has not revealed an abundance of spine processes on embryos 14-18 days of incubation.

The avian NL has been considered by some to be the homologue of the mammalian MSO (Boord, '69; Ramón y Cajal, '71). In many ways the correspondences between these nuclei are striking, including similar electrophysiological response properties (Goldberg and Brown, '68, '69; Schwartzkopff, '68; Guinan et al., '72; Rubel and Parks, '75) and afferent innervation (Stotler, '53; Goldberg and Brown, '68; Boord, '68; van Noort, '69; Strominger and Strominger, '71; Parks and Rubel, '75). The gross cellular and dendritic orgnizations of these nuclei also correspond, as both nuclei are laminar and composed largely of cells with bipolar dendritic orientations (Ramón y Cajal, '71). Recent Golgi studies of the dendritic structure of the MSO by the Scheibels ('74) and by Schwartz ('77) have revealed, however, that the MSO possesses a great deal more complexity in its organization than does NL. Examination of sagittal sections of the MSO of the cat has indicated that the dendrites of the bipolar cells extend not only in the medial-to-lateral dimension (as they are usually portrayed in coronal sections, cf. Ramón y Cajal, '71: fig. 345) but also in the anterior-to-posterior plane, often for considerable distances (Morest, '73; Scheibel and Scheibel, '74). Thus, the dendrites of these cells can be only incompletely appreciated in one plane of section, and they present considerable obstacles to quantification. These observations of dendritic anisotropy in the MSO have been confirmed by Schwartz ('77),

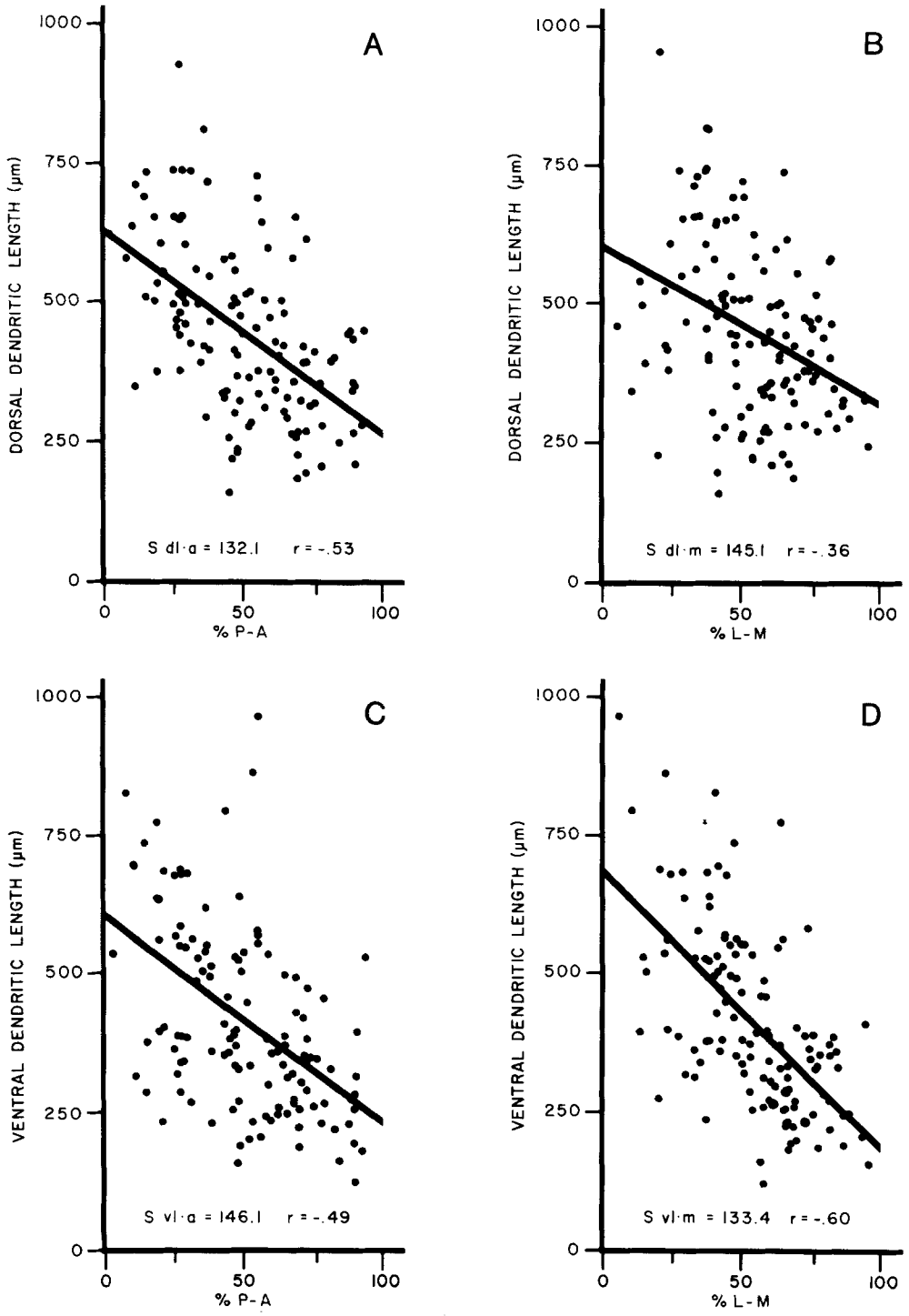

Fig. 17 Scatterplots and regressions relating dorsal and ventral dendritic lengths to position in each dimension of NL. The standard errors of estimate and correlation coefficients are shown. A. Relationship of dorsal dendritic length to the posterior-to-anterior dimension of NL. (Regression equation for dorsal dendritic length = −3.58 (%P-A) + 630). B. Relationship of dorsal dendritic length to the lateral-to-medial position in NL. (Regression equation for dorsal dendritic length = −2.74 (%L-M) + 599). The correlation of dorsal length with the L-M dimension is reliably less than with the P-A dimension, ($p < 0.05$). C. Relationship of ventral dendritic length with the posterior-to-anterior dimension of NL. (Regression equation for ventral length = −3.59 (%P-A) + 590). D. Relationship of ventral dendritic length with the lateral-to-medial dimension of NL. (Regression equation for ventral dendritic length = −5.01 (%L-M) + 682). It can be seen that for the ventral dendrites the higher correlation is along the latero-medial dimension ($p < 0.05$). ($n = 125$ in all cases.)

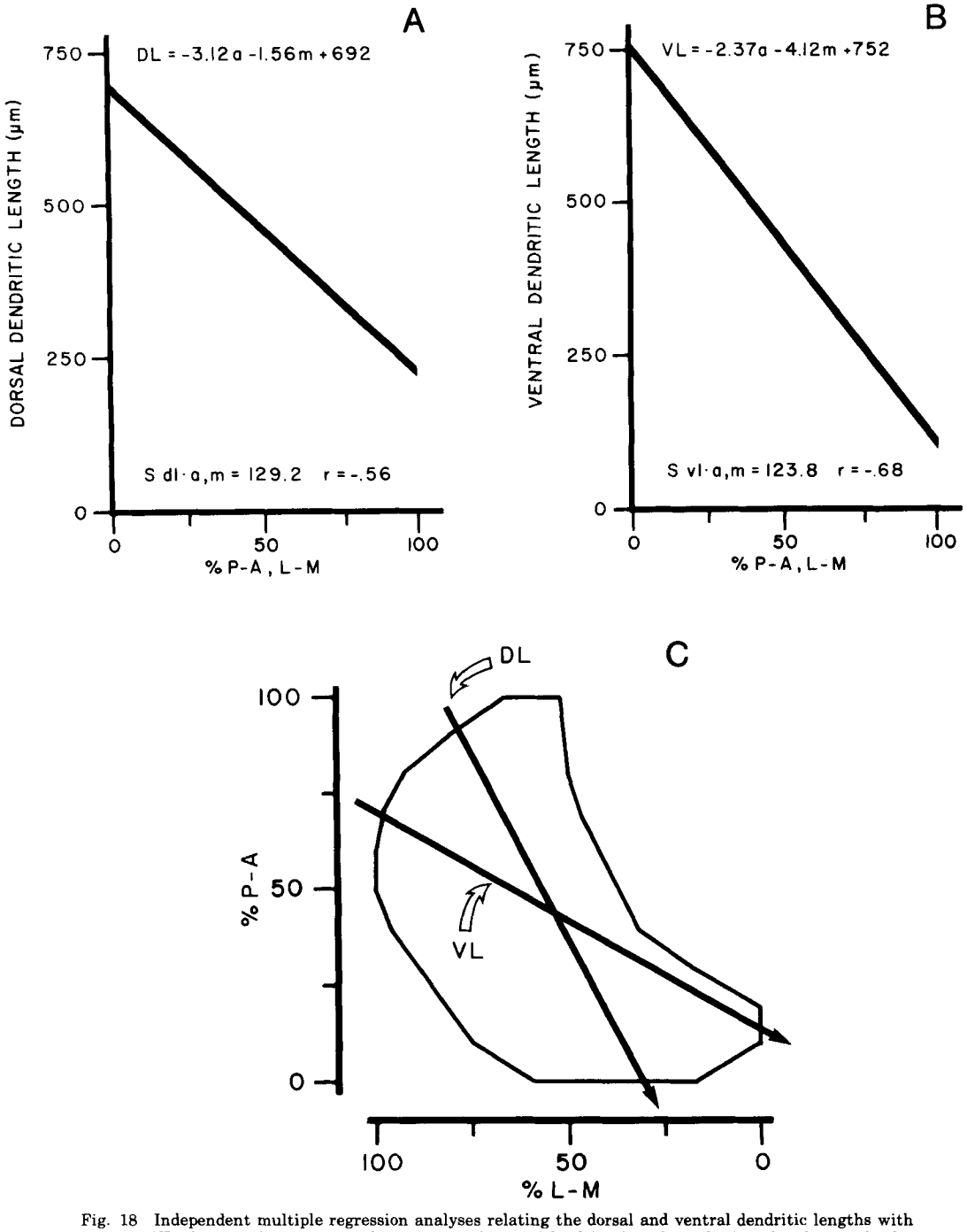

Fig. 18 Independent multiple regression analyses relating the dorsal and ventral dendritic lengths with position in NL, showing the existence of separate gradients of dendritic length on the dorsal and ventral sides of the nucleus. A. Multiple linear regression of dorsal dendritic length on both the posterior-to-anterior and lateral-to-medial axes of NL. The regression equation (top), standard error of estimate, and correlation coefficient are shown. (n = 125). B. Multiple linear regression relating ventral dendritic length to the positional variables for NL. The regression equation, standard error of estimate, and correlation coefficient are shown. (n = 125). C. Planar projection of NL, across which has been plotted the gradients of increase for dorsal dendritic length (DL) and for ventral dendritic length (VL), as derived from the multiple regression equations in A and B. The two gradients are divergent.

who found that the number of dendritic fibers perpendicular to the plane of the MSO was equalled by the number parallel to it, resulting in an encirclement of the MSO by dendritic processes. Observations of sagittal sections of NL have not revealed a similar anisotropy of dendritic orientation; in both the sagittal and coronal planes the appearance of NL cells is nearly identical. Eighty-five percent of the area of NL is occupied by cells with dendritic orientations perpendicular to the plane of the nucleus; only the caudolateral 15% is occupied by cells whose dendrites branch to form a canopy of processes parallel to the plane of the nucleus. These processes rarely extend more than 200 μm in the anterior-posterior or mediolateral planes. Schwartz ('77) also found a variety of cell types other than bipolar cells in the MSO. Beside the bipolar cell, the only other cell type reminiscent of that seen in NL is the marginal cell, which may be somewhat analogous to the NL perilaminar drapery-like cell described above.

In sum, similarities in afferent and cytostructural organizations of the MSO and of NL suggest that the nuclei are involved in a similar processing of auditory information, probably related to sound localization (Goldberg and Brown, '69; Erulkar, '72; Parks and Rubel, '75; Jenkins and Masterson, '79). In this regard, it is interesting to note that drawings from Golgi sections of the mammalian MSO often depict it as though it had a similar gradient of dendritic morphology (Morest, '73: fig. 3; Ramón y Cajal, '71: fig. 345). However, as mentioned, the 3-dimensional extent of the MSO neurons makes this difficult to assess. Although the significance, if any, of the relationship of dendritic morphology to the frequency organization of NL (and possibly MSO) is presently unclear, two approaches which may be particularly fruitful in elucidating its meaning are a comparative analysis of NL, relating it to behavioral specializations (as has been done for the MSO, Masterson et al., '75), or an electrotonic analysis of the properties of NL's dendrites (e.g., Rall, '77). The comparative simplicity of NL suggests it may be easier to analyze the function of these nuclei in the avian system.

Implications of dendritic structure in NL for dendritic ontogeny

There are obvious limitations and dangers associated with any attempt to infer the developmental history of a structure from analysis of a single time point. On the other hand, the morphological gradients in NL do impose sharp constraints on ontogenetic hypotheses; any hypotheses which are incapable of explaining the dendritic gradients in NL must be rejected. In this way, the thorough analysis of a structure at any point in time does provide clues to the causal mechanisms which shape it. Ultimately the power of inferential arguments about the ontogeny of dendritic structure resides largely in their ability to predict dendritic structure in this and other systems. In this case, the simple and unique dendritic structure of NL makes particularly clear which of a number of explanatory hypotheses can meet the requirements of NL's structure. The hypotheses formed can later be directly evaluated by the observation and manipulation of ontogenetic events in the nucleus.

At the age examined in this study (5 days posthatch) NL has not yet assumed all the aspects of cellular morphology which characterize it in the adult chicken. It is highly unlikely, however, that all of the gradients described are simply the result of incomplete development of the nucleus. By five days posthatch, the chick auditory system has been functionally competent for nearly two weeks, as determined by behavioral responses in ovo to sound stimulation (Jackson and Rubel, '78; Rubel, '78), by recorded responses of NL cells to 8th nerve stimulation *in vitro* (Jackson, Hacket and Rubel, unpublished observations), and by *in vivo* electrophysiological responses (Saunders et al., '73). These and other indices of development in this system (Rubel, Smith and Miller, '76) confirm the impression gained from observation of older animals that the major ontogenetic events in NL have already occurred by the time point examined herein. Finally, a preliminary qualitative and quantitative examination of NL in older animals (25 days posthatch) has revealed little significant change in the directions or orientations of the gradients of dendritic size or number from those described herein (Smith and Rubel, unpublished observations).

Hypotheses which can be invoked to account for the regulation of dendritic size and number may be classed into two broad categories: those postulating regulation intrinsic to the neurons; and those postulating extrinsic controls. The extrinsic milieu of neurons is such that hypotheses about extrinsic regulation are limited to three further classes, in-

cluding control by substances in the extracellular space, control by the glia, and control by the afferents. Within each of the above classes there are any number of specific, mechanistic hypotheses which could be offered, and which will not be discussed. Our data speak only to the above broad classes of hypotheses, and each will be examined in turn.

The first class of ontogenetic hypotheses holds that the control of dendritic size is intrinsic to each neuron. The observed gradient of total dendritic size or number would then result from a gradient of somatic differentiation. A corollary of exclusively intrinsic control of the dendritic parameters is that the regulation is on a cell-by-cell basis. Three points argue that this hypothesis is not in accord with our observations of NL. First, the correlation of the dorsal and ventral dendritic sizes on a cell-by-cell basis explains only 22% of the variance found in dendritic size ($r = 0.47$, fig. 15), while the amount of variance that is accounted for by either the dorsal or ventral gradients is significantly greater. This implies that NL neurons would have to be more effective in between-cell coordination of dendritic growth than in within-cell coordination. This is a clear contradiction of any hypothesis postulating predominantly intrinsic control of dendritic size. Second, the dorsal and ventral dendritic gradients are not the same (fig. 18). If the information controlling the dendritic growth were to reside within the cells, it would be then necessary to divide it into dorsal and ventral components. The aforementioned paradox of coordination of the gradients is thereby exacerbated by now demanding separate coordination of growth across the dorsal and ventral halves of the cells. Third, the very close regulation of the dorsal and ventral dendritic lengths within the isofrequency zones ($r = 0.93$, fig. 16) is also more compatible with inter- than with intracellular regulation. Thus, the comparatively small amount of variance in dendritic form which can be accounted for under the condition of within-cell control of dendritic ontogeny makes it unlikely that such control is the major factor determining NL's dendritic morphology. Moreover, it is quite difficult to envision how intrinsic control could account for the separate dorsal and ventral morphological gradients.

This leads to the evaluation of possible extrinsic factors which may account for the largest portion of variance in dendritic size. Three of the most reasonable classes of ontogenetic hypotheses are those postulating control by a diffusible substance or morphogen (Wolpert, '71; Meinhardt, '78); those invoking control by the glia; and those postulating control by the afferents.

The gradients of dendritic structure in NL are extremely difficult to reconcile with hypotheses of control by a gradient of some diffusible substance. In order to account for the separate dorsal and ventral gradients of the dendritic parameters, such a substance must be postulated to diffuse differentially over the dorsal and ventral surfaces of a nucleus which is generally one cell (and at most a few cells) thick. Accepting this premise, the edge of NL initially contacted by such an external diffusant would have an approximately equal concentration of the factor on the dorsal and ventral sides of the nucleus. Hence, the dorsal and ventral dendritic sizes would be most nearly equal in this area, with the gradients progressing away from it. Solving the regression equations for equality of the dorsal and ventral dendritic lengths (fig. 18) reveals that the area where their values are equals along the rostrolateral edge of NL. A diffusant controlling dendritic size must then have been a gradient from rostrolateral to caudomedial across NL: this is, however, at right angles to the observed overall gradient (rostromedial to caudolateral). Thus, it is not likely that the control of dendritic size is exercised by a morphogen gradient, even granting such a substance the ability to diffuse differentially over the dorsal and ventral sides of NL.

Each of the two remaining classes of hypotheses, which are regulation by the glia and by the afferents to NL, imply that intercellular contacts are the critical regulators of dendritic size and number. Since both the glial cell bodies and the afferents are segregated on either side of NL (Parks and Rubel, '75; Rubel et al., '76), it would appear that either factor is well placed to account for the separate dorsal and ventral dendritic gradients. Further observation of Golgi-impregnated material reveals, however, that the processes of a given glia cell do not remain exclusively on one side of the nucleus; 30%-50% of them extend through NL, terminating or ramifying on the other side. This is also the case in embryonic tissue (Smith and Rubel, unpublished observations). To the degree that glial processes in

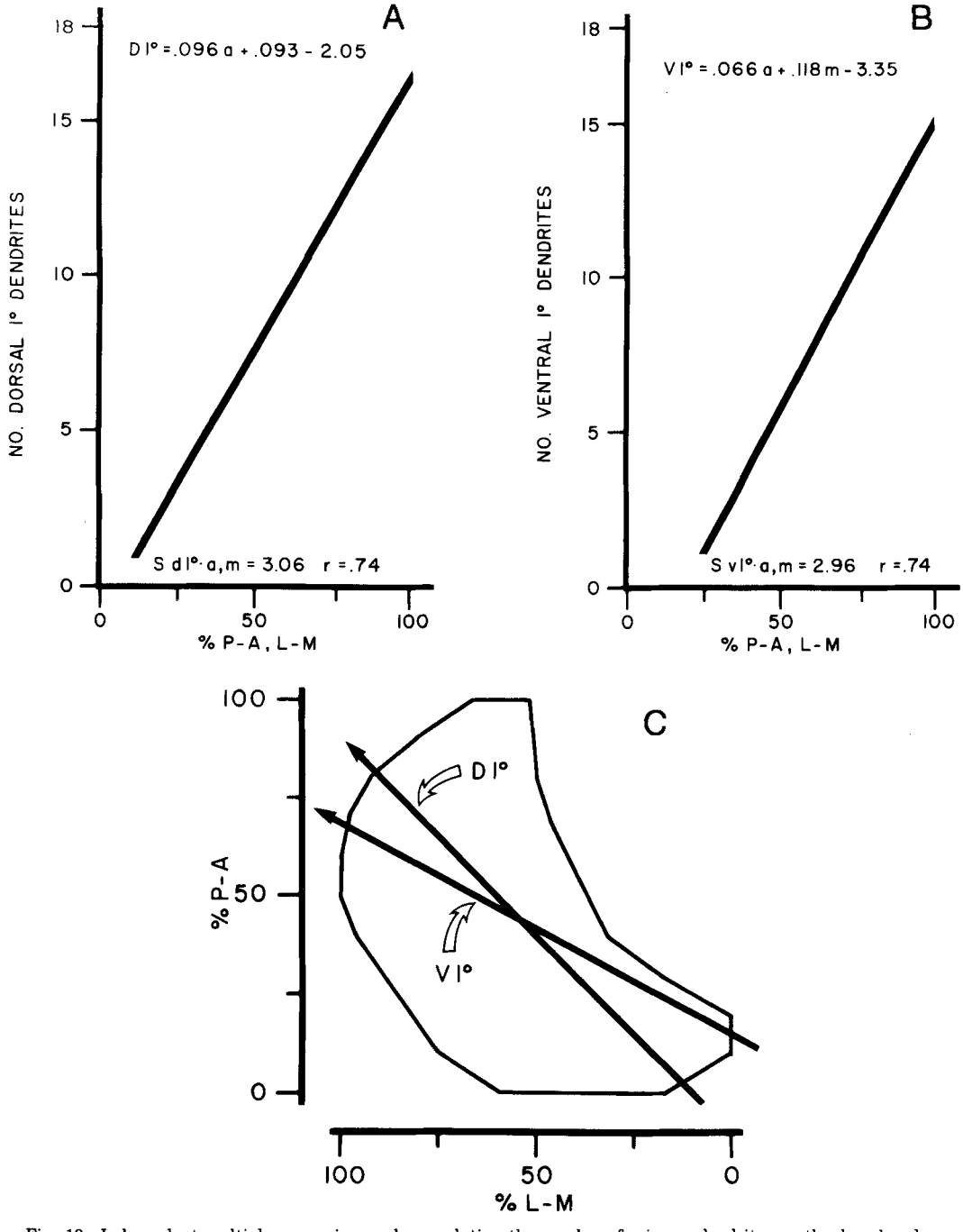

Fig. 19 Independent multiple regression analyses relating the number of primary dendrites on the dorsal and ventral sides of NL with position in the nucleus, showing the existence of separate gradients of dendrite number on the dorsal and ventral sides of NL. A. Multiple linear regression relating the number of dorsal primary dendrites (D1°) with position in both dimensions of the nucleus. The regression equation, standard error of estimate, and correlation coefficient are shown. (n = 122). B. Multiple linear regression relating the number of ventral primary dendrites (V1°) with position in both dimensions of NL. The regression equation, standard error of estimate, and correlation coefficient are shown. (n = 122). C. Planar projection of NL, across which has been plotted the dorsal and ventral gradients of increase of primary dendrites. The two gradients are divergent.

the dorsal and ventral neuropil areas overlap, it is difficult to attribute to them a role in shaping the dorsal and ventral gradients. Although the class of hypotheses which postulates glial control of dendritic development may not be ruled out to the degree that those invoking somatic or diffusible-morphogen control can be, there is to our knowledge little or no experimental or theoretical reason to propose such glial control, nor is it clear there would be further explanatory or predictive value in such a proposal. Perhaps the observed distribution of glial cell bodies in NL results from their preferential association with the tips of growing dendrites, as has been observed with embryonic chick neurons in vitro (Grainger and James, '70).

The dendritic structure of NL, therefore, provides logical contradictions to ontogenetic hypotheses involving either somatic differentiation or a diffusible-substance gradient as the principal factors regulating dendritic size, and regulation by the glia seems unlikely. Instead, the two major observations of highly related dorsal and ventral dendritic sizes on an area-by-area basis (fig. 16), and separable overall gradients for the dorsal and ventral dendrites, require that a regulatory factor must influence growth on areal basis *and* differentially act on the dorsal and ventral dendritic surfaces. These requirements point to the afferent input to NL as an important source of regulation. Further evidence for this conclusion converges from a number of observations. First, the principal and only inputs to NL are the tonotopic, bilateral projections from the magnocellular nuclei (Boord, '68; Parks and Rubel, '75, '78; Rubel and Parks, '75; Benes et al., '77). Our observation that the gradients of total dendritic length and number coincide closely with the frequency gradient in NL (fig. 14) suggests a causal relationship between the dendritic parameters and the afferents to NL. Second, both cell death and lamina formation follow a similar rostromedial-to-caudolateral developmental time course (Rubel et al., '76). Silver-staining indicates that the arrival of afferents to NL also follows a spatio-temporal gradient similar to the final gradient of length and number in this nucleus (Smith and Rubel, unpublished observations). Lastly, preliminary observations from in vitro electrophysiological experiments suggest that the same gradient may be followed by the functional development of the afferents to NL (Jackson, Hackett and Rubel, unpublished). In all cases, the rostromedial region is first differentiated.

The hypothesis that afferents are responsible for the control of dendritic size can also account for the separate dorsal and ventral gradients of length, as well as the overall gradient orientation. The spatial segregation of ipsilateral and contralateral afferents to the dorsal and ventral dendrites, respectively, of NL, coupled with the relatively weak coordination of dendritic size on the dorsal and ventral sides of NL cells (fig. 15), logically suggest the existence of separate gradients on the two sides of NL. The different orientations of these gradients could result from different spatio-temporal gradients of the arrival of the afferents to the two sides of the nucleus. Consonant with this interpretation are observations from Golgi-stained material (Jhaveri, '78) and our own laboratory's observations of HRP-filled NM cells showing the ipsilateral afferents approach NL along a primarily rostrocaudal trajectory while contralateral NM projections follow a primarily mediolateral trajectory across NL. Finally, the premise that dendritic size is regulated on an areal basis by NM afferents (to account for high dorsal-ventral area correlation, fig. 16B) requires that the NM projections average their input over an area of NL. Consistent with this interpretation, recent results from in vitro analysis of embryonic brain stem (Jackson et al., '78; Rubel et al., '78) show a high degree of convergence and divergence of the NM projections onto NL.

Numerous previous studies have demonstrated that the development and maintenance of dendritic size and structure are dependent upon an intact afferent supply (e.g., Globus, '75; Benes et al., '77; Kimmel et al., '77; Smith, '77). As this principle becomes accepted, more attention is being paid to possible mechanisms of afferent regulation of postsynaptic structure (Perry and Cronly-Dillon, '78; Stewart and Rose, '78). Whatever the precise mechanisms, an important component is probably the amount or pattern of activity of the afferents (Tanzi, 1893; Coleman and Risesen, '68; Uylings et al., '78; Rutledge, '78; Borges and Berry, '78; Pittman and Oppenheim, '78). Unfortunately, in most neural systems it is difficult or impossible to specify the amount of afferent activity available to the cell or class of cells of interest in situa-

tions where it has presumably been manipulated (Rodieck, '67; Sakakura and Iwama, '67; Valverde, '67; Hubel and Wiesel, '70; Guillery, '72; Sherman et al., '72; Globus, '73; Greenough et al., '73; Kasamatsu and Adey, '74; Sherman and Stone, '74; Bradley and Berry, '76; Yoon, '76; Sherman, '77; Borges and Berry, '78; Burke and Cole, '78). NL and nucleus magnocellularis may be unusually amenable to the determination of the effects of afferent activity on dendritic ontogeny. The amount of afferent activity can be determined by rate-intensity functions (Møller, '72; Kiang et al., '73) and thereby directly controlled, and the tonotopicity of these nuclei, along with the limited diversity and spatial segregation of inputs to NL, allows control by the stimulus of the specific neural elements activated.

ACKNOWLEDGMENTS

The authors are grateful to D. Kent Morest and Sonal Jhaveri for demonstrating impregnation of NL cells by the Stensaas procedure; Lincoln Gray for statistical assistance; Thomas Parks, Hunter Jackson and Oswald Steward for critical readings of the manuscript; Marilyn Engelhardt and Eleanor Hardin for able secretarial assistance. Some of the histological material used for qualitative examination was provided by Thomas Parks. Supported by NSF Grant BNS78-04074, funds from the Deafness Research Foundation, and NIH predoctoral fellowship F31 MH05949. The data in this paper are to be included in a dissertation presented at the University of Virginia.

LITERATURE CITED

Benes, F. M., T. N. Parks and E. W Rubel 1977 Rapid dendritic atrophy following deafferentation: an EM morphometric analysis. Brain Res., *120:* 1-13.

Berry, M., and P. M. Bradley 1976a The application of network analysis to the study of branching patterns of large dendritic fields. Brain Res., *109:* 111-132.

——— 1976b The growth of the dendritic trees of Purkinje cells in the cerebellum of the rat. Brain Res., *112:* 1-35.

Berry, M., T. Hollingsworth, R. M. Flinn and E. M. Anderson 1972 Dendritic field analysis: a reappraisal. TIT J. Life Sci., *2:* 129-140.

Bock, W. J. 1969 The origin and radiation of birds. Ann. N.Y. Acad. Sci., *167:* 147-155.

Bok, S. T. 1959 Histonomy of the Cerebral Cortex. Elsevier, Amsterdam.

Boord, R. L. 1961 The efferent cochlear bundle in the caiman and the pigeon. Exp. Neurol., *3:* 225-239.

——— 1968 Ascending projections of the primary cochlear nuclei and nucleus laminaris in the pigeon. J. Comp. Neur., *133:* 523-542.

——— 1969 The anatomy of the avian auditory system. Ann. N.Y. Acad. Sci., *167:* 147-155.

Boord, R. L., and G. L. Rasmussen 1963 Projection of the cochlear and lagenar nerves on the cochlear nuclei of the pigeon. J. Comp. Neur., *120:* 463-475.

Borges, S., and M. Berry 1976 Preferential orientation of stellate cell dendrites in the visual cortex of the dark-reared rat. Brain Res., *112:* 141-147.

——— 1978 The effects of dark rearing on the development of the visual cortex of the rat. J. Comp. Neur., *180:* 277-300.

Bradley, P., and M. Berry 1976 The effects of reduced climbing and parallel fibre input on Purkinje cell dendritic growth. Brain Res., *109:* 133-151.

Burke, W., and A. M. Cole 1978 Extraretinal influences on the lateral geniculate nucleus. Rev. Physiol. Biochem. Pharmacol., *80:* 105-166.

Coleman, P. D., and A. Riesen 1968 Environmental effects on cortical dendritic fields. I. Rearing in the dark. J. Anat., *102:* 363-374.

Eayrs, J. T. 1955 The cerebral cortex of normal and hypothyroid rats. Acta Anat., *25:* 160-183.

Eayrs, J. T., and B. Goodhead 1959 Post-natal development of the cerebral cortex in the rat. J. Anat., *93:* 385-407.

Erulkar, S. D. 1972 Comparative aspects of spatial localization of sound. Physiol. Rev., *52*(1): 237-360.

Gelfan, S., G. Kao, and D. S. Ruchkin 1970 The dendritic tree of spinal neurons. J. Comp. Neur., *139:* 385-412.

Globus, A. 1975 Brain morphology as a function of presynaptic morphology and activity. In: The Developmental Neuropsychology of Sensory Deprivation. A. H. Riesen, ed. Academic Press, New York, pp. 9-91.

Globus, A., M. R. Rosenzweig, E. L. Bennett and M. C. Diamond 1973 Effects of differential experience on dendritic spine counts in rat cerebral cortex. J. Comp. Physiol. Psychol., *82:* 175-181.

Goldberg, J. M., and P. B. Brown 1968 Functional organization of the dog superior olivary complex: an anatomical and electrophysiological study. J. Neurophysiol., *31:* 639-656.

——— 1969 Response of binaural neurons of dog superior olivary complex to dichotic tonal stimuli: some physiological mechanisms of sound localization. J. Neurophysiol., *32:* 613-636.

Gottlieb, G. 1971 Development of Species Identification in Birds: An Inquiry into the Prenatal Determinants of Perception. University of Chicago Press, Chicago.

——— 1976 Early development of species-specific auditory perception in birds. In: Studies on the Development of Behavior and the Nervous System. G. Gottlieb, ed. Academic Press, New York. Vol. 3. pp. 237-280.

Grainger, F., and D. W. James 1970 Association of glial cells with the terminal parts of neurite bundles extending from chick spinal cord in vitro. Z. Zellforsch., *108:* 93-104.

Greenough, W. T., F. R. Volkmar and J. M. Juraska 1973 Effects of rearing complexity on dendritic branching in frontolateral and temporal cortex of the rat. Exp. Neurol., *41:* 371-378.

Guillery, R. W. 1972 Binocular competition in the control of geniculate cell growth. J. Comp. Neur., *144:* 117-129.

Guinan, J. J., S. S. Guinan and B. E. Norris 1972 Single auditory units in the superior olivary complex. I. Responses to sounds and classification based on physiological properties. Int. J. Neurosci., *4:* 101-120.

Hinde, R. A. 1969 Bird Vocalizations in Relation to Current Problems in Biology and Psychology. Cambridge University Press, Cambridge.

Hinds, J. W., and N. A. McNelly 1977 Aging of the rat olfactory bulb: growth and atrophy of constituent layers and changes in size and number of mitral cells. J. Comp. Neur., *171:* 345-368.

Hirokawa, N. 1978 Synaptogenesis in the basilar papilla of the chick. J. Neurocytol., *7:* 283-300.

Hubel, D. H., and T. N. Wiesel 1970 The period of susceptibility to the physiological effects of unilateral eye closure in kittens. J. Physiol., *(London), 206:* 419-436.

Jackson, H., J. T. Hackett and E. W Rubel 1978 *In vitro* electrophysiological analysis of n. magnocellularis and n. laminaris of the chicken. Neurosci. Abst., *4:* 7.

Jackson, H., and E. W Rubel 1978 Ontogeny of behavioral responsiveness to sound in the chick embryo as indicated by electrical recordings of motility. J. Comp. Physiol. Psychol., *92:* 680-694.

Jenkins, W. M., and R. B. Masterson 1979 Sound localization in pigeon *(Colomba livia).* J. Comp. Physiol. Psychol., in press.

Jhaveri, S. R. 1978 Morphogenesis in the Auditory System of the Chicken: A Study of Nucleus Magnocellularis. Doctoral dissertation, Harvard University.

Karten, H. J. 1967 Organization of the ascending auditory pathway in the pigeon *(Columbia livia).* I. Diencephalic projections of the inferior colliculus (nucleus mesencephalicus lateralis, pars dorsalis). Brain Res., *6:* 409-427.

——— 1968 The ascending auditory pathway in the pigeon *(Columba livia).* II. Telencephalic projections of the nucleus ovoidalis thalami. Brain Res., *11:* 134-153.

Kasamatsu, T., and W. R. Adey 1974 Immediate effects of total visual deafferentation on single unit activity in the visual cortex of freely behaving cats. I. Tonic excitability changes. Exp. Brain Res., *20:* 157-170.

Kerr, L. M., M. Ostapoff and E. W Rubel 1979 The influence of acoustic experience on the ontogeny of frequency generalization gradients in the chicken. J. Exp. Psychol.: Anim. Behav. Proc., *5:* 97-115.

Kiang, N. Y. S., D. K. Morest, D. A. Godfrey, J. J. Guinan and E. C. Kane 1973 Stimulus coding at caudal levels of the cat's auditory nervous system. I. Response characteristics of single units. In: Basic Mechanisms in Hearing. A. Møller, ed. Academic Press, New York, pp. 455-578.

Kimmel, C. B, E. Shabtach and R. J. Kimmel 1977 Developmental interactions in the growth and branching of the lateral dendrite of Mauthner's cell *(Ambystoma mexicanum).* Devel. Biol., *55:* 244-259.

Konishi, M. 1970 Comparative neurophysiological studies of hearing and vocalizations in songbirds. Z. Vergl. Physiol., *66:* 257-272.

——— 1973 Development of auditory neuronal responses in avian embryos. Proc. Nat. Acad. Sci., *70:* 1795-1798.

Leibler, L. 1975 Monaural and Binaural Pathways in the Ascending Auditory System of the Pigeon. Doctoral dissertation, MIT.

Leppelsack, H. J., and M. Vogt 1976 Resonses of auditory neurons in the forebrain of a songbird to stimulation with species-specific sounds. J. Comp. Physiol., *107:* 263-274.

Levi-Montalcini, R. 1949 Development of the acusticovestibular centers in the chick embryo in the absence of the afferent root fibers and of descending fiber tract. J. Comp. Neur., *91:* 209-242.

Mannen, H. 1966 Contribution to the morphological study of dendritic arborization in the brain stem. Prog. Brain Res., *21A:* 131-162.

Marler, P. 1970 A comparative approach to vocal learning: song development in white-crowned sparrows. J. Comp. Psychol., *71:* 1-25.

Marler, P., and M. S. Waser 1977 Role of auditory feedback in canary song development. J. Comp. Physiol. Psychol., *91:* 8-16.

Masterton, B., G. C. Thompson, J. K. Bechtold and M. J. RoBards 1975 Neuroanatomical basis of binaural phase-difference analysis for sound localization: A comparative study. J. Comp. Physiol. Psychol., *89:* 379-386.

McConnell, P., and M. Berry 1978a The effects of undernutrition on Purkinje cell dendritic growth in the rat. J. Comp. Neur., *177:* 159-172.

——— 1978b The effect of refeeding after neonatal starvation on Purkinje cell dendritic growth in the rat. J. Comp. Neur., *178:* 759-772.

Meinhardt, H. 1978 Models for the ontogenetic development of higher organisms. Rev. Physiol. Biochem. Pharmacol., *80:* 47-104.

Møller, A. R. 1972 Coding of amplitude and frequency modulated sounds in the cochlear nucleus of the rat. Acta Physiol. Scand., *81:* 540-556.

Morest, D. K. 1973 Auditory neurons of the brain stem. Adv. Oto-Rhino-Laryng., *20:* 337-356.

Nauta, W. J. H., and H. J. Karten 1970 A general profile of the vertebrate brain, with sidelights on the ancestry of the cerebral cortex. In. The Neurosciences: Second Study Program. F. O. Schmitt, ed. Rockefeller University Press, New York, pp. 7-26.

Parks, T. N. 1979 Afferent influences on the development of the brain stem auditory nuclei of the chicken: Otocyst ablation. J. Comp. Neur., *183:* 665-678.

Parks, T. N., and E. W Rubel 1975 Organization and development of brain stem auditory nuclei of the chicken: Organization of projections from n. magnocellularis to n. laminaris. J. Comp. Neur., *164:* 435-448.

——— 1978 Organization and development of the brain stem auditory nuclei of the chicken: Primary afferent projections. J. Comp. Neur., *180:* 43-448.

Perry, G. W., and J. R. Cronly-Dillon 1978 Tubulin synthesis during a critical period in visual cortex development. Brain Res., *142:* 374-378.

Pittman, R. H., and R. W. Oppenheim 1978 Neuromuscular blockade increases motoneuron survival during normal cell death in the chick embryo. Nature, *271:* 364-366.

Rall, W. 1977 Core conductor theory and cable properties of neurons. In: Handbook of Physiology, Sect. 1, Vol. 1. E. Kandel, ed. Am. Physiol. Soc., Bethesda, pp. 39-97.

Ramón y Cajal, S. 1908 Les ganglions terminaux du nerf acoustique des oiseaux. Trab. Inst. Cajal Invest. Biol., *6:* 195-224.

——— 1971 (The Acoustic Nerve: its cochlear branch or cochlear nerve.) Translated from: Histologie du Systéme Nerveux de l'Homme et des Vertebrés. Tome I, pp. 774-838, 1952. National Technical Information Service Publication #PB 205 473.

Rodieck, R. W. 1967 Maintained activity of cat retinal ganglion cells. J. Neurophysiol., *30:* 1043-1071.

Rubel, E. W 1978 Ontogeny of structure and function in the vertebrate auditory system. In: Handbook of Sensory Physiology, Vol. IX, Development of Sensory Systems. M. Jacobson, ed. Springer-Verlag, New York, pp. 135-237.

Rubel, E. W, H. Jackson and J. T. Hackett 1978 In vitro analysis of synaptic potentials and neuronal morphology in avian brain stem auditory nuclei. J. Acoust. Soc. Am., *64:* Suppl. 1, (386).

Rubel, E. W, and T. N. Parks 1975 Organization and development of brain stem auditory nuclei of the chicken: Tonotopic organization of n. magnocellularis and n. laminaris. J. Comp. Neur., *164:* 411-434.

Rubel, E. W, T. N. Parks, D. J. Smith and H. Jackson 1979 Experiential afferent influences and development in the

avian n. magnocellularis and n. laminaris. Proc. XVII Intern. Cong. Ornithol., in press.

Rubel, E. W, and M. Rosenthal 1975 The ontogeny of auditory frequency generalization in the chicken. J. Exp. Psychol.: Anim. Behav. Proc., *1:* 287-297.

Rubel, E. W, D. J. Smith and L. C. Miller 1976 Organization and development of brain stem auditory nuclei of the chicken: Ontogeny of n. magnocellularis and n. laminaris. J. Comp. Neur., *166:* 469-490.

Rutledge, L. T. 1978 Effects of cortical denervation and stimulation on axons, dendrites, and synapses. In: Neuronal Plasticity. C. Cotman, ed. Raven Press, New York, pp. 273-289.

Sachs, M. B., R. H. Lewis and E. D. Young 1974 Discharge patterns of single fibers in the pigeon auditory nerve. Brain Res., *70:* 431-447.

Sachs, M. B., and J. M. Sinnott 1978 Responses to tones of single cells in nucleus magnocellularis and nucleus angularis of the Redwing Blackbird *(Agelaius phoeniceus).* J. Comp. Physiol., *126:* 347-361.

Sakakura, H., and K. Iwama 1967 Effects of bilateral eye enucleation upon single unit activity of the lateral geniculate body in free behaving cats. Brain Res., *6:* 667-678.

Samuels, M. L., J. E. Mittenthal, G. P. McCabe and P. D. Coleman 1977 Complexity of branching in dendritic trees: dependence on number of trees per cell and effects of branch loss during sectioning. J. Anat., *124:* 701-715.

Saunders, J. C., R. B. Coles and G. R. Gates 1973 The development of auditory evoked responses in the cochlea nuclei of the chick. Brain Res., *63:* 59-74.

Scheibel, M. E., and A. B. Scheibel 1974 Neuropil organization in the superior olive of the cat. Exp. Neurol., *43:* 339-348.

Scheich, H., G. Langner and R. Koch 1977 Coding of narrow-band and wide-band vocalizations in the auditory midbrain (MLD) of the guinea fowl *(Numida meleagris).* J. Comp. Physiol., *117:* 245-265.

Schwartz, I. R. 1977 Dendritic arrangements in the cat medial superior olive. Neurosci., *2:* 81-101.

Schwartzkopff, J. 1968 Structure and function of the ear and of the auditory brain areas in birds. Proc. XIII Intern. Ornithol. Congr., *2:* 1059-1068.

Sherman, S. M. 1977 The effect of superior colliculus lesions upon the visual fields of cats with cortical ablations. J. Comp. Neur., *172:* 211-320.

Sherman, S. M., K. P. Hoffman and J. Stone 1972 Loss of a specific cell type from dorsal lateral geniculate nucleus in visually deprived cats. J. Neurophysiol., *35:* 532-541.

Sherman, S. M., and J. Stone 1973 Physiological normality of the retina in the visually deprived cat. Brain Res., *60:* 224-230.

Sholl, D. A. 1953 Dendritic organization in the neurons of the visual and motor cortices of the cat. J. Anat., *87:* 387-407.

Smith, D. E. 1977 The effect of deafferentation on the development of brain and spinal nuclei. Prog. Neurobiol., *8:* 349-367.

Stensaas, L. J. 1967 The development of hippocampal and dorsolateral pallial regions of the cerebral hemisphere in fetal rabbits. I. Fifteen millimeter stage, spongioblast morphology. J. Comp. Neur., *129:* 59-70.

Stewart, M. G., and S. P. R. Rose 1978 Increased binding of [^{3}H-]colchicine to visual cortex proteins of dark-reared cats on first exposure to light. J. Neurochem., *30:* 595-599.

Stotler, W. A. 1953 An experimental study of the cells and connections of the superior olivary complex of the cat. J. Comp. Neur., *98:* 401-423.

Strominger, N. L., and A. I. Strominger 1971 Ascending brain stem projections of the anteroventral cochlear nucleus in the rhesus monkey. J. Comp. Neur., *143:* 217-242.

Tanzi, E. 1893 I fatti e le induzioni nell'odierna istologia del sistema nervosa. Riv. Sperim. Frenat., *19:* 419-472.

Tyner, C. F. 1975 The naming of neurons: applications of taxonomic theory to the study of cellular subpopulations. Brain Behav. and Evol., *12;* 75-96.

Uylings, H. B. W., K. Kuypers, M. C. Diamond and W. A. M. Veltman 1978 Effects of differential environments on plasticity of dendrites of cortical pyramidal neurons in adult rats. Exp. Neurol., *62:* 658-677.

Valverde, F. 1967 Apical dendritic spines of the visual cortex and light deprivation in the mouse. Exp. Brain Res., *3:* 337-352.

van Noort, J. 1969 The structure and connections of the inferior colliculus. In: An Investigation of the Lower Auditory System. Van Gorcum, Leiden.

Vince, M. A. 1969 Embryonic communication, respiration and the synchronization of hatching. In: Bird Vocalizations. R. A. Hinde, ed. Cambridge University Press, Cambridge, pp. 233-260.

Wolpert, L. 1971 Positional information and pattern formation. Curr. Top. Dev. Biol., *6:* 183-224.

Woolf, N. K., J. L. Bixby and R. R. Capranica 1976 Prenatal experience and avian development: brief auditory stimulation accelerates the hatching of Japanese quail. Science, *194:* 959-960.

Yoon, C. H. 1976 Pleiotropic effects of the staggerer gene. Brain Res., *109:* 206-215.